American Mineralogist, Volume 94, pages 1293–1311, 2009

Evolution of uranium and thorium minerals

Robert M. Hazen,[1,*] Rodney C. Ewing,[2] and Dimitri A. Sverjensky[1,3]

[1]Geophysical Laboratory, Carnegie Institution of Washington, 5251 Broad Branch Road NW, Washington, D.C. 20015, U.S.A.
[2]Department of Geological Sciences, University of Michigan, 1100 North University Avenue, Ann Arbor, Michigan 48109-1005, U.S.A.
[3]Department of Earth and Planetary Sciences, Johns Hopkins University, Baltimore, Maryland 21218, U.S.A.

Abstract

The origins and near-surface distributions of the ~250 known uranium and/or thorium minerals elucidate principles of mineral evolution. This history can be divided into four phases. The first, from ~4.5 to 3.5 Ga, involved successive concentrations of uranium and thorium from their initial uniform trace distribution into magmatic-related fluids from which the first U^{4+} and Th^{4+} minerals, uraninite (ideally UO_2), thorianite (ThO_2), and coffinite ($USiO_4$), precipitated in the crust. The second period, from ~3.5 to 2.2 Ga, saw the formation of large low-grade concentrations of detrital uraninite (containing several wt% Th) in the Witwatersrand-type quartz-pebble conglomerates deposited in a highly anoxic fluvial environment. Abiotic alteration of uraninite and coffinite, including radiolysis and auto-oxidation caused by radioactive decay and the formation of helium from alpha particles, may have resulted in the formation of a limited suite of uranyl oxide-hydroxides.

Earth's third phase of uranium mineral evolution, during which most known U minerals first precipitated from reactions of soluble uranyl $(U^{6+}O_2)^{2+}$ complexes, followed the Great Oxidation Event (GOE) at ~2.2 Ga and thus was mediated indirectly by biologic activity. Most uraninite deposited during this phase was low in Th and precipitated from saline and oxidizing hydrothermal solutions (100 to 300 °C) transporting $(UO_2)^{2+}$-chloride complexes. Examples include the unconformity- and vein-type U deposits (Australia and Canada) and the unique Oklo natural nuclear reactors in Gabon. The onset of hydrothermal transport of $(UO_2)^{2+}$ complexes in the upper crust may reflect the availability of $CaSO_4$-bearing evaporites after the GOE. During this phase, most uranyl minerals would have been able to form in the O_2-bearing near-surface environment for the first time through weathering processes. The fourth phase of uranium mineralization began ~400 million years ago, as the rise of land plants led to non-marine organic-rich sediments that promoted new sandstone-type ore deposits.

The modes of accumulation and even the compositions of uraninite, as well as the multiple oxidation states of U (4+, 5+, and 6+), are a sensitive indicator of global redox conditions. In contrast, the behavior of thorium, which has only a single oxidation state (4+) that has a very low solubility in the absence of aqueous F-complexes, cannot reflect changing redox conditions. Geochemical concentration of Th relative to U at high temperatures is therefore limited to special magmatic-related environments, where U^{4+} is preferentially removed by chloride or carbonate complexes, and at low temperatures by mineral surface reactions.

The near-surface mineralogy of uranium and thorium provide a measure of a planet's geotectonic and geobiological history. In the absence of extensive magmatic-related fluid reworking of the crust and upper mantle, uranium and thorium will not become sufficiently concentrated to form their own minerals or ore deposits. Furthermore, in the absence of surface oxidation, all but a handful of the known uranium minerals are unlikely to have formed.

Keywords: Uranium, thorium, mineral evolution, ore deposits, geobiology

Introduction

The mineralogy of terrestrial planets and moons has undergone sequential changes as physical, chemical, and biological processes modified the initially relatively homogeneous material of the nascent solar nebula into differentiated zones of varied temperature, pressure, and composition (Hazen et al. 2008). Earth's 4.5 billion year history can be thus divided into 10 stages of mineral evolution (Table 1), each of which saw changes in the planet's near-surface mineralogy. The pre-solar molecular cloud contained approximately a dozen micro- and nano-scale refractory minerals that represent the starting point of Earth's mineral evolution. Gravitational clumping into a protoplanetary disk, star formation, and the resultant heating in the stellar nebula produced primary refractory constituents of chondritic meteorites with ~60 different mineral phases. Subsequent aqueous, thermal, and shock alteration of chondrites coupled with asteroidal accretion and differentiation led to ~250 different minerals that are still found in unweathered meteorite samples.

Following planetary accretion and differentiation, the initial mineral evolution of Earth's crust depended on a sequence of geochemical and petrologic processes, including volcanism and

* E-mail: rhazen@ciw.edu

Table 1. Ten stages of Earth's mineral evolution, with possible timing and estimates of the cumulative number of different mineral species

Stage	Age (Ga)	~Cumulative no. species
1. Primary chondrite minerals	>4.56 Ga	60
2. Achondrite and planetesimal alteration	>4.56 to 4.55 Ga	250
3. Igneous rock evolution	4.55 to 4.0 Ga	350 to 500*
4. Granite and pegmatite formation	4.0 to 3.5 Ga	1000
5. Plate tectonics	>>3.0 Ga	1500
6. Anoxic biological world	3.9 to 2.5 Ga	1500
7. Great Oxidation Event	2.5 to 1.9 Ga	>4000
8. Intermediate ocean	1.9 to 1.0 Ga	>4000
9. Snowball Earth events	1.0 to 0.542 Ga	>4000
10. Phanerozoic era of biomineralization	0.542 Ga to present	4300+

Note: Note that the timings of some of these stages overlap, and several stages continue to the present (after Hazen et al. 2008).
* Depending on the volatile content of the planet or moon.

Table 2. Estimated U and Th content in different Earth reservoirs

Reservoir	U (ppm)	Th (ppm)	References
CI carbonaceous chondrites	0.0074	0.02*	Plant et al. (1999)
Eucrite meteorites	0.07 to 0.15	0.3 to 0.8	T. McCoy and L. Nittler, pers. com.
Bulk silicate Earth	0.02	0.06*	Plant et al. (1999); Palme and O'Neill (2003)
Crust	1 to 2.7	~10	Taylor (1964); Plant et al. (1999); Emsley (1991)
MORB	0.05 to 0.15	~0.15 to 0.45	Lundstrom (2003); Workman and Hart (2004)
OIB	1	3*	Plant et al. (1999)
Granite	10	30	Plant et al. (1999)
High-grade ore deposits	10^4 to 10^5	10^4	Plant et al. (1999); Deer et al. (1997)
Average seawater	3×10^{-3}	9×10^{-6}	Miyake et al. (1970); Emsley (1991); Chen and Wasserburg (1986)
Average river water	$\sim 10^{-4}$	$\sim 2.5 \times 10^{-4}$	Bertine et al. (1970); Moore (1967); Windom et al. (2000)

*Estimated from known U concentration and average U:Th ~ 1:3.

degassing, fractional crystallization, crystal settling, assimilation reactions, regional and contact metamorphism, plate tectonics, and associated large-scale fluid-rock interactions. These processes produced the first continents with their associated near-surface granitoids and pegmatites, hydrothermal ore deposits, high-pressure metamorphic terrains, evaporites, and zones of surface weathering, and resulted in an estimated 1500 different mineral species. According to some origin-of-life scenarios, a planet must progress through at least some of these stages of chemical processing as a prerequisite for life (Hazen 2005).

Biological processes began to affect Earth's mineralogy by the Eoarchean (~3.9 Ga; stage 6), when large-scale near-surface mineral deposits were precipitated under the influences of changing atmospheric and ocean chemistry. The Paleoproterozoic "Great Oxidation Event" (~2.2 to 2.0 Ga; stage 7), when atmospheric oxygen may have risen to >1% of modern levels, and additional Neoproterozoic increases in atmospheric oxygen following at least two major glaciation events, ultimately gave rise to multicellular life and skeletal biomineralization and irreversibly transformed Earth's surface mineralogy (stages 9 and 10). Biochemical processes may thus be responsible, directly or indirectly, for most of Earth's ~4300 known mineral species.

The concept of mineral evolution places mineralogy in a dynamic historical context, in which different species arise at different stages of planetary history. However, the initial presentation of this framework by Hazen et al. (2008) did not examine any one group of minerals in detail. Here the objective is to elucidate principles of mineral evolution by focusing on the origin and near-surface distribution of ~250 known uranium and/or thorium minerals (Finch and Murakami 1999; Lauf 2008; http://rruff.info/ima/), which demonstrate rich and varied parageneses. The element uranium is particularly instructive in this regard for at least five reasons: (1) U is a trace element (~2 to 3 ppm in Earth's crust; Table 2) and thus it illustrates modes of element migration and concentration; (2) U occurs in two common valence states of contrasting behavior, 4+ and 6+, as well as the less common 5+ state (Burns and Finch 1999a; Schindler et al. 2009), and thus highlights the role of near-surface redox gradients in mineral diversification; (3) U is an element of considerable technological importance and environmental concern, so physical properties, thermochemical parameters, and phase equilibria of uranium minerals, aqueous species, and surface species have been intensively studied (Frondel 1958; Garrels and Christ 1959; Langmuir 1978; Hemingway 1982; Vochten and Van Haverbeke 1990; Grenthe et al. 1992; Waite et al. 1994; Shock et al. 1997a; Burns and Finch 1999b; Bourdon et al. 2003; Guillaumont et al. 2003); (4) U mineralogy is modified both directly and indirectly through microbial and other biological activity, and thus underscores the mineralogical co-evolution of Earth's geo- and biospheres (Suzuki and Banfield 1999); and (5) the neutronic properties of ^{235}U are such that natural fission and associated neutron-capture reactions can lead to the addition of transuranium elements to crustal abundances [e.g., ~3 metric tons (mT) of Pu at the Oklo natural reactors, 5 mT of Pu from atmospheric testing of nuclear weapons, and 1800 mT of Pu from nuclear power reactors]. In addition, the gradual transition of U to radiogenic Pb in uranium minerals leads to a variety of intriguing and idiosyncratic alteration behaviors (Finch and Ewing 1992a).

The story of thorium's mineral evolution provides an instructive complement to that of uranium, because the elements are quite similar in the crystal chemistry of their relatively insoluble 4+ valence states, but Th does not adopt the distinctive highly soluble 6+ valence state of U. In addition, Th^{4+} and U^{4+} in aqueous solution show significant differences in aqueous complexing: $Th^{4+}_{(aq)}$ is mobilized under much more restricted circumstances than $U^{4+}_{(aq)}$.

These two elements, U and Th, are a unique pair in the periodic chart and of special importance to geoscientists. Uranium and thorium are the most massive two naturally occurring elements (not counting the extremely low contemporary crustal concentrations of a few of the other heavy elements, e.g., Pa and Pu), and the most abundant of the actinide series. The energy released by the radioactive decay of U and Th has driven Earth's thermal evolution, resulting in Earth's layered internal structure and the continued movement of plates across Earth's surface. The radioactive decay of ^{238}U, ^{235}U, and ^{232}Th also provides the rich array of radiogenic elements, such as radon, that occur in the three naturally occurring radioactive decay chains. The decay

to stable isotopes of Pb provides the basis for geochronological measurements that added absolute dates to the geologic time scale at the beginning of the 20th century (Holmes 1911). The fields of fission-track dating (Wagner and Van den Haute 1992) and thermochronology (Reiners et al. 2005) depend on the nuclear processes of spontaneous fission and the formation of He by alpha-decay. Departures from secular equilibrium in the decay-chains can be caused by a wide variety of geologic processes, and thus provide the foundation for the field of uranium-series geochemistry (Crisp 1984; Sleep 1990; Bourdon et al. 2003; Bourdon and Sims 2003; Turner et al. 2003). Uranium and thorium are the fundamental resource for nuclear power. ^{235}U is fissile, ^{238}U can be used to "breed" ^{239}Pu that is fissile, and ^{232}Th can be used to "breed" fissile ^{233}U. The fate of these actinides and their fission products are central to the new field of environmental radiochemistry (Santschi and Honeyman 1989; Eisenbud and Gesell 1997) and the issue of expanded nuclear power and the proliferation of nuclear weapons.

We elaborate on the outline of Nash et al. (1981), who examined changes in the type and distribution of uranium ore deposits since the Archean. More than 220 different uranium minerals have been described, but uranium mineralogy is dominated volumetrically by uraninite (ideally UO_2). Therefore, the history of uranium mineralization, including its diversification and distribution, is closely linked to ore deposits. In this review, observations of ore deposits over time provide one key to understanding U and Th mineral evolution.

Nash et al. (1981) and Cuney and Kyser (2009) propose that the evolution of uranium ore deposits on Earth can be divided into four principal phases. The first period, encompassing the Hadean and earlier Archean eons (~4.5 to 3.5 Ga), involved successive concentration of both U and Th from their initial uniform trace distribution to highly enriched magmatic fluids, where they were incorporated as minor elements in zircon (which can concentrate U relative to Th). Subsequent fluid enrichment led to the first uranium minerals, predominantly uraninite and coffinite (ideally $USiO_4$).

The second phase of U mineral evolution, from ~3.5 to 2.2 Ga, saw the formation of detrital Th-bearing uraninite in Witwatersrand-type quartz-pebble conglomerates deposited in an anoxic surface environment. Abiotic alteration of uraninite and coffinite, including the remarkable process of "auto-oxidation" by which radioactive decay leads to the formation of daughter products, such as Pb, and the formation of He from alpha-particles, may have resulted in the formation of a limited suite of uranyl oxide-hydroxides and other uranyl species.

The third phase of uranium mineral evolution on Earth, during which the great majority of uranium minerals first appeared, followed the Great Oxidation Event (GOE) at ~2.2 Ga and thus was indirectly caused by biological processes. This phase saw the deposition of low-Th uraninite from saline and oxidizing hydrothermal solutions (100 to 300 °C), which transported uranium in the 6+ oxidiation state as $(UO_2)^{2+}$ complexes. Examples include unconformity- and vein-type U deposits (Australia and Canada) and the unique Oklo natural nuclear reactors in Gabon. During this phase, most uranyl minerals would have been able to form through weathering processes in the O_2-bearing near-surface environment. Subsequent changes in near-surface uranium mineralogy have been strongly influenced by microbial activity, both indirectly through changes in atmospheric chemistry, and directly through passive uranium sequestration and U-coupled redox metabolism.

The rise of land plants ~400 million years ago led to a fourth phase of uranium mineral deposition, as low-temperature, oxygenated, U-rich near-surface waters precipitated uraninite and coffinite at reduction fronts in organic-rich continental sediments. The resulting sandstone-type ore deposits hold a significant fraction of known uranium reserves in the United States and Australia. The uranium deposits of the western United States are predominantly roll front deposits, whose distinctive curving shape is controlled by the movement of groundwater through coarse-grained sandstones.

The modern period of "technogenic" nuclear evolution of U and Th, though not treated in detail here, represents a fifth and final phase. The development of nuclear reactors for electric power generation (providing ~15% of the world's electricity) relies on the use of fissile ^{235}U. The production and testing of nuclear weapons (reaching a peak of more than 70000 in the 1980s) requires the enrichment of ^{235}U or the production of ^{239}Pu in nuclear reactors. Both of these activities have created new inventories of transuranium elements, such as plutonium (>1800 metric tons created in nuclear reactors). The geochemical signature of enhanced crustal concentrations of fission product and transuranium elements created by nuclear reactions provides a clear record of the nuclear activities of the 20th century (Ewing 1999).

Stellar synthesis of the heavy elements

The most abundant elements in the universe are H and He, mostly formed during the first minutes of the Big Bang. During the subsequent formation of stars, nuclear processes lead to the formation of Fe, Ni, and other moderately heavy elements, but much heavier elements, such as ^{235}U, ^{238}U, and ^{232}Th, are formed only in the span of a few seconds during the explosion of supernovae, when the flux of free neutrons is greatest (Tolstikhin and Kramers 2008). The post-supernovae ratio of U to Th is similar to modern terrestrial abundances (Th is ~3× as abundant as U), but the combined abundance of these elements is 12 orders of magnitude less than hydrogen. Each of these nuclides is unstable and decays by spontaneous fission or radioactive decay along chains that form a series of daughter product elements by alpha- and beta-decay events. A fourth chain, headed by ^{237}Np, has disappeared because of the relatively short half-life of ^{237}Np (~2.1 million years). Crustal abundances for Earth are greater than the cosmic abundances, reflecting the early chemical differentiation of these lithophile elements (Table 2). Uranium and thorium crustal concentrations are comparable to those of the rare earth elements and greater than those of Hg, Au, and Bi.

Phase I—Uranium and thorium concentration (~4.5 to 3.5 Ga)

Uranium and thorium are trace elements, with estimated whole-Earth concentrations of >10 and ~30 ppb, respectively (Table 2). Therefore, before any U or Th minerals can form, the elements must be transported and concentrated locally by many orders of magnitude. The geochemistry of U and Th during Phase I was dominated by the 4+ oxidation state in magmas and in

aqueous solutions. For example, Figure 1 shows the conditions required for equal activities of representative aqueous U^{4+} and U^{6+} species in the system U-O-H (Shock et al. 1997a; Murphy and Shock 1999) at neutral pH values. The figures indicate that the uranium 4+ oxidation state should predominate in such solutions buffered by fayalite-magnetite-quartz (FMQ), pyrrhotite-pyrite-magnetite (PPM), or magnetite-hematite (MH) at temperatures as high as 1000 °C. The more soluble U^{6+} might become important only under relatively oxidizing conditions and preferential complexing relative to U^{4+}. The solubility of thorianite can be expected to be similar to the low solubility of uraninite in the absence of complexing ligands.

The key to understanding uranium and thorium concentration mechanisms in this phase of Earth history lies in their crystal-chemical and aqueous-solution behaviors. In its reduced 4+ valence state, uranium's ionic radius is 0.89 and 1.00 Å (corresponding to U-O distances of ~2.25 and ~2.36 Å) in 6- and 8-coordination, respectively. These values are similar to those of Th^{4+} (ionic radii 0.94 and 1.05 Å and Th-O distances ~2.30 and 2.41 Å in 6- and 8-coordination, respectively), which explains the similar crystal chemistries of U^{4+} and Th^{4+}. Uranium and thorium are highly incompatible in all common rock-forming silicates except for zircon ($ZrSiO_4$), which can accommodate several weight percents of the isostructural coffinite ($USiO_4$) or thorite ($ThSiO_4$) end-members (Deer et al. 1997; Blundy and Wood 2003). The world's oldest known zircon grains from the Jack Hills district in Western Australia have U and Th concentrations of up to hundreds of parts per million with Th/U ratios as low as 0.59. In addition, U^{4+} and Th^{4+} may enter the structures of several phosphates, niobates, tantalates, and titanates, including minerals of the apatite, monazite, pyrochlore, samarskite, and columbite groups (Burns 1999; Finch and Murakami 1999), but these U- and Th-enriched phases must have been rare or nonexistent prior to the first formation of complex pegmatites in the Mesoarchean Era (London 2008).

A consequence of the distinctive crystal-chemical behavior of uranium and thorium, coupled with their trace chondritic abundance of <10 and <30 ppb, respectively, was that no discrete U or Th minerals appear to have formed in any meteorites (mineral evolution stages 1 and 2; Table 1). Rather, U and Th are present in meteorites as widely dispersed elements, perhaps concentrating in interstitial regions (T. McCoy and L. Nittler, personal communications).

Three mechanisms contributed to uranium and thorium mobility and segregation in primitive terrestrial planets and moons. First, U and Th were initially concentrated into low-density, Si-rich melt phases and thus were fractionated into the crust, with enrichment factors of at least 100 compared with the mantle. This fractionation process is underscored by analyses of eucrites (basaltic meteorites), which are found to contain 70 to 150 ppb U and 300 to 800 ppb Th (T. McCoy and L. Nittler, personal communications)—an order of magnitude enrichment compared with chondrites. Mid-ocean ridge basalts (MORB), similarly, are found to contain 50–150 ppb U and ~3× as much Th (Table 2). Thus, while igneous processes led to zircon grains significantly enriched in U and Th, planetary differentiation and the formation of a basaltic veneer appear to be inadequate to concentrate these elements sufficiently to promote the precipitation of discrete mineral phases in which uranium or thorium are essential elements. We conclude that it is unlikely that any such minerals could have formed solely through the agencies of differentiation or igneous processes on volatile-poor worlds, such as the Moon or Mercury. Furthermore, it is unlikely that U and Th would be separated geochemically in the absence of the involvement of key aqueous complexes in the magmatic processes (Keppler and Wyllie 1990).

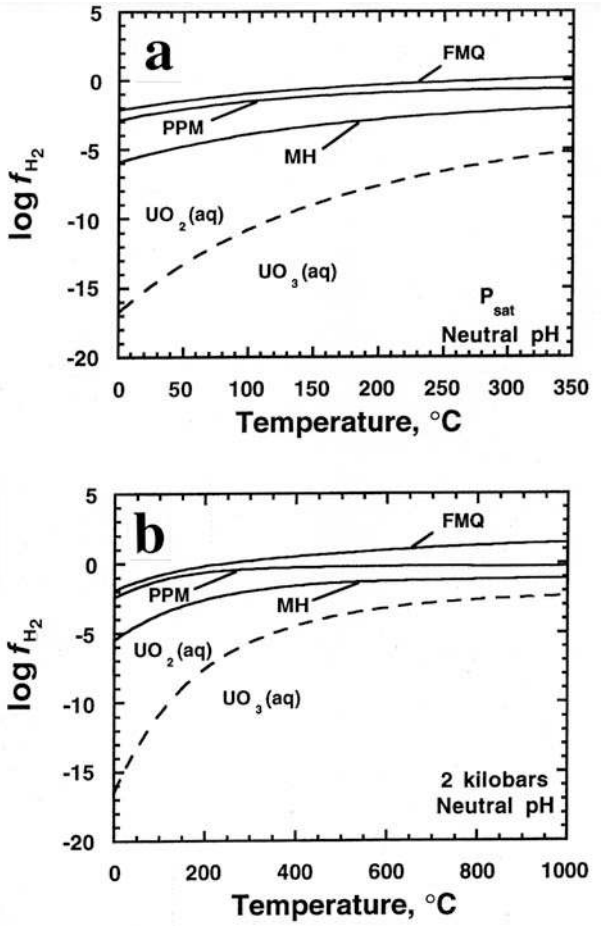

FIGURE 1. Relative predominance fields for reduced and oxidized uranium in aqueous solutions in the system U-O-H (dashed lines) compared with the oxidation states defined by mineral buffers represented by the solid lines (after Shock et al. 1997a): (**a**) at 1 atmosphere and (**b**) at 0.2 GPa (2 kbar).

Magmatic hydrothermal activity provided a second mechanism that further concentrated uranium and probably thorium during Earth's first billion years, as well as enabling efficient geochemical separation of the two. Uraninite is highly insoluble as the U^{4+} species $UO_{2(aq)}$ in aqueous solutions with pH > 3 and at temperatures up to about 300 °C (Shock et al. 1997a). But U^{4+} dissolves readily at low pH (< ~4) in the presence of fluoride that forms soluble U^{4+}-F complexes (Langmuir 1978) at 25 °C (Fig. 2). It can be expected that such complexes will be even more effective at elevated temperatures and moderate pressures and that similar considerations should apply to Th^{4+}-F complexes (Keppler and Wylie 1990). Thus, reduced U and Th could have become enriched in Earth's crustal residual fluids associated with

granitization, especially alkaline and/or peraluminous granites formed by the partial melting of arkosic sediment wedges, and particularly if significant amounts of F were present. These granites commonly contain 10 ppm U, which is a factor of 100 greater than MORB (Table 2) and 30 ppm Th. Separation of U from Th under these circumstances can be expected to occur if chloride- or CO_2-rich fluids become involved in magmatic processes because complexing of U^{4+} by chloride or carbonate is apparently much stronger than for Th^{4+} at elevated temperatures and pressures (Keppler and Wyllie 1990). The first uranium mineralization may have occurred when magmatic-derived fluids influenced by chloride and/or carbonate, instead of fluoride, mixed with cooler, neutral-pH meteoric water to precipitate uraninite (ideally UO_2, though see below). Whatever thorium remained should follow uranium under such situations, so that uraninite crystals precipitated from magmatic-related fluids typically contain significant quantities of Th, up to about 12 wt% ThO_2 (Frondel 1958; Finch and Murakami 1999), although clearly U has been greatly enriched in such systems relative to Th compared with crustal igneous source rocks (Fig. 3).

A third important mechanism for uranium mineralization, which has led to the largest U ore deposits since the Paleoproterozoic Eon (<2.5 Ga), relies on U in the 6+ oxidation state. If near-surface U^{4+} becomes oxidized, for example through UV photo-oxidation, auto-oxidation, or near-surface oxidative weathering, the resulting uranyl complexes are highly soluble. Uranyl minerals can then form directly at Earth's surface by evaporation. Furthermore, if these uranyl-bearing solutions intersect a subsurface redox boundary where soluble U^{6+} is converted to insoluble U^{4+}, then uraninite (or coffinite in the case of some environments with high SiO_2 activity) will be deposited at the boundary. However, while this mechanism plays a central role in the formation of many post-Archean U ore bodies, no economic hydrothermal uranium deposits formed from $(UO_2)^{2+}$-bearing solutions are known from the Archean (Plant et al. 1999). Similarly, uranium-enriched potassic sub-alkaline to alkaline granites, which may host complex pegmatites with uranium mineralization, do not appear until the Paleoproterozoic (London 2008).

One implication of these observations is that the necessary enrichment factor of at least 10^6 for U mineral precipitation required perhaps a billion years or more for extensive fluid reworking of the upper mantle and crust. Indeed, it is possible that the added hydrothermal vigor associated with plate tectonic processes was essential to foster sufficient fluid circulation to enrich the crust in radioactive elements, for example at spreading centers in fractionated basalt and in hydrated mantle wedges above subduction zones. If so, then there may not be any significant U mineralization on Mars or Venus. In any event, it seems likely that uranium mineralization did not first occur on Earth until at least stage 4 of mineral evolution, if not stage 5 (Table 1). Consequently, theories for life's origin that rely on significant concentration of radionuclides (e.g., Adam 2007) appear to be untenable.

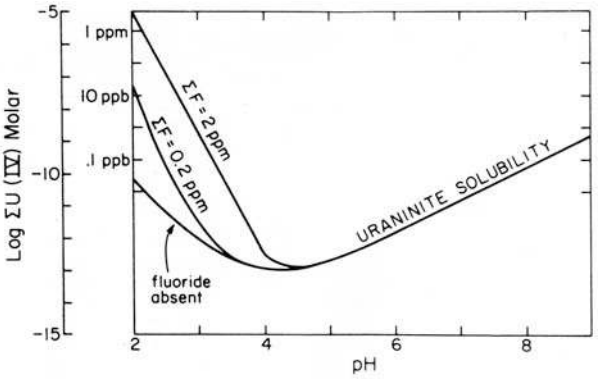

Figure 2. A plot of pH vs. uraninite solubility (from Langmuir 1978) reveals that uraninite solubility increases by several orders of magnitude in acidic aqueous fluoride solutions. Such mobilization of U^{4+} complexes was a primary mechanism of U enrichment prior to the Great Oxidation Event.

A note on plutonium mineral evolution

Plutonium was not a geochemically significant element for most of Earth's history. However, primordial ^{244}Pu (half-life ~82 million years) might have played a geochemical role during Earth's first billion years. Turner et al. (2004) cite evidence for the presence of this extinct isotope at an estimated initial abundance $^{244}Pu/^{238}U \sim 0.0066$, based on measurements of zircons (4.2 to 4.1 Ga) from Jack Hills, Australia. Pu^{4+} forms the oxide PuO_2, which is isostructural with uraninite; thus, uraninite might have hosted trace amounts of plutonium on the early Earth. However, lacking an efficient concentration mechanism or sufficient time, no plutonium minerals are likely to have formed in Earth's early history.

Figure 3. Uraninite crystal (1 cm in length) with feldspar from the Swamp Mine, Maine. Uraninite crystals precipitated from magmatic-related fluids typically contain significant quantities of Th, up to about 12 wt% ThO_2, although U has been greatly enriched in such systems relative to Th compared with crustal igneous source rocks. Photo courtesy of Robert Lauf. Crystal is 1.5 cm tall.

Phase II—Detrital uraninite accumulation and abiotic alteration (~3.5 to 2.2 Ga)

The oldest known major accumulations of uranium are detrital uraninite grains concentrated in the Witwatersrand quartz-pebble conglomerates in South Africa. Uraninite occurs throughout the succession of siliciclastic sediments, which range in age from 3.074 to 2.714 Ga in association with gold. Although the grade of the uranium ore is only about 300 ppm, these deposits may represent Earth's largest uranium resource (Frimmel 2005). Occurrences of detrital uraninite grains are also found in Mesoarchean (3.2 to 2.8 Ga) sediments from the Australian Pilbara Craton and Indian Bhima Group, and in the Paleoproterozoic Canadian Blind River deposits (2.4 to 2.2 Ga). Ore deposits of detrital uraninite grains in fluvial sedimentary rocks are not found in younger successions. These examples indicate a worldwide occurrence of uraninite that must have eroded from preexisting U-bearing bodies into active stream environments during the period 3.2 to 2.7 Ga. Uraninite weathers relatively rapidly in an oxygen-rich atmosphere, so the fact that uraninite grains were transported in fluvial environments during this period has been cited as one of several lines of evidence for an essentially anoxic surface environment at that time (Grandstaff 1980; Holland 1984, 1994; Fareeduddin 1990; Prasad and Roscoe 1996; Rasmussen and Buick 1999; England et al. 2002; Kumar and Srinivasan 2002; Frimmel 2005).

The most thoroughly studied of the detrital uraninite deposits is the Witwatersrand succession (Frimmel 2005; Pretorius 1981; Frimmel and Minter 2002). Despite long-standing controversies over the relative importance of detrital sedimentary vs. hydrothermal processes in the origin of the uranium and the gold in these deposits, substantial evidence supports a modified placer origin (Frimmel 2005). Textural, isotopic, and compositional characteristics of the uraninite, gold, and pyrite in the deposits strongly point to original deposition as detrital grains along with the host siliciclastic sediments. These characteristics include rounded particles indicative of stream transport, isotopic dating indicating ages older than the sedimentary host rocks, and in the case of the rounded uraninite grains a great variation in the Th/U ratios with average values of 3.9 wt% Th, indicating a variety of sedimentary provenances and granitic to pegmatitic source rocks (Frimmel 2005). In contrast, hydrothermal uraninite could be expected to have uniformly low Th concentrations (Finch and Murakami 1999). Hydrothermal alteration and metamorphism have undoubtedly affected the Witwatersrand succession and the distribution of uraninite, gold, and pyrite, but these effects can be interpreted as superimposed on the placer deposits. It is interesting to note that detrital pyrite and uraninite, as well as siderite, have also been described in Archean fluvial sedimentary rocks in the Pilbara, which do not contain ore deposits and have not been subject to hydrothermal alteration or as much metamorphism as the Witwatersrand rocks (Rasmussen and Buick 1999).

It therefore appears that important characteristics of this second phase of uranium and thorium mineral evolution are the widespread occurrences of detrital uraninite and the Th-rich composition of the uraninite. Consequently, the major mechanism for concentration of U and Th during this phase involves weathering of preexisting uraninite of granitic or pegmatitic origin and transport and deposition in siliciclastic sediments under anoxic near-surface conditions. Near-surface redox conditions during the Archean remain uncertain (Catling and Claire 2005). However, if it is accepted that uraninite did not weather under near-surface conditions because there was no thermodynamic driving force, then thermochemical data may be used to place constraints on these conditions. For example, we used thermodynamic data from Shock et al. (1997a, 1997b), Chen et al. (1999), and Finch and Murakami (1999) to calculate $\log f_{O_2}$-pH diagrams at 25 °C and 1 bar illustrating the conditions under which uraninite would either dissolve to $(UO_2)^{2+}_{(aq)}$ or be altered to uranyl minerals (Fig. 4). More recent calorimetric and solubility studies (Kubatko et al. 2005, 2006; Gorman-Lewis 2007) will permit consideration of additional uranyl minerals when entropies as well as enthalpies are measured experimentally. As emphasized by Finch and Murakami (1999), the uncertainties in the standard Gibbs free energies of the uranyl minerals are likely to be substantial. However, the diagrams consistently show that there is no thermodynamic driving force for the alteration of uraninite for f_{O_2} values less than about 10^{-45} bars at 25 °C. It should be noted that if aqueous complexing of $(UO_2)^{2+}_{(aq)}$ takes place, the stability field of $(UO_2)^{2+}_{(aq)}$ would expand relative to the minerals. Consequently, the f_{O_2} upper limit for uraninite stability could be less than 10^{-45} bars. Although very low, such values are in fact consistent with the persistence of detrital pyrite and siderite in rocks of this period (Lee et al. 2008). Similarly, the lack of mobility of U, and limited mobility of Mo and Re, during weathering processes in the source region for the 2.5 Ga Mount McRae Shale from Western Australia (Anbar et al. 2007) is also consistent with redox-pH conditions in the uraninite field and the aqueous molybdate and rhenate fields (Fig. 5).

Despite the apparent stability of uraninite under near-surface conditions, some diversification of uranium mineralogy probably occurred as early as the Mesoarchean Era. For example, the U^{4+} minerals coffinite and brannerite [$(U,Ca,Ce)(Ti,Fe)_2O_6$], which are also present in Archean ore bodies, would have formed as a consequence of the reaction of hot reducing fluids with UO_2 (Nash et al. 1981; Smits 1989; Dahlkamp 1993; Fayek and Kyser 1997; Cuney and Kyser 2009). It is also likely that a limited suite of uranyl (U^{6+}) minerals formed in spite of the absence of an oxidizing environment as a consequence of gradual oxidative alteration of uraninite through the radiogenic production of helium nuclei (alpha particles) and conversion of uranium to lead—a process known as "auto-oxidation."

Uraninite auto-oxidation

^{238}U, which now constitutes 99.3% of U isotopes, undergoes radioactive decay with a half-life of 4.46×10^9 years. The ultimate stable decay product, after a chain of more than a dozen intermediate steps, is ^{206}Pb (Bourdon et al. 2003). Thus, uraninite steadily accumulates Pb—ultimately, as much as 20 atom percent replacing U. Lead is incompatible with uraninite's fluorite-type structure (Janeczek and Ewing 1995), so this gradual chemical change leads to at least five types of alteration. These and other uraninite alteration mechanisms have been studied extensively because UO_2 is a principal component of nuclear fuel rods and its alteration is a principal concern in the handling of spent nuclear fuel.

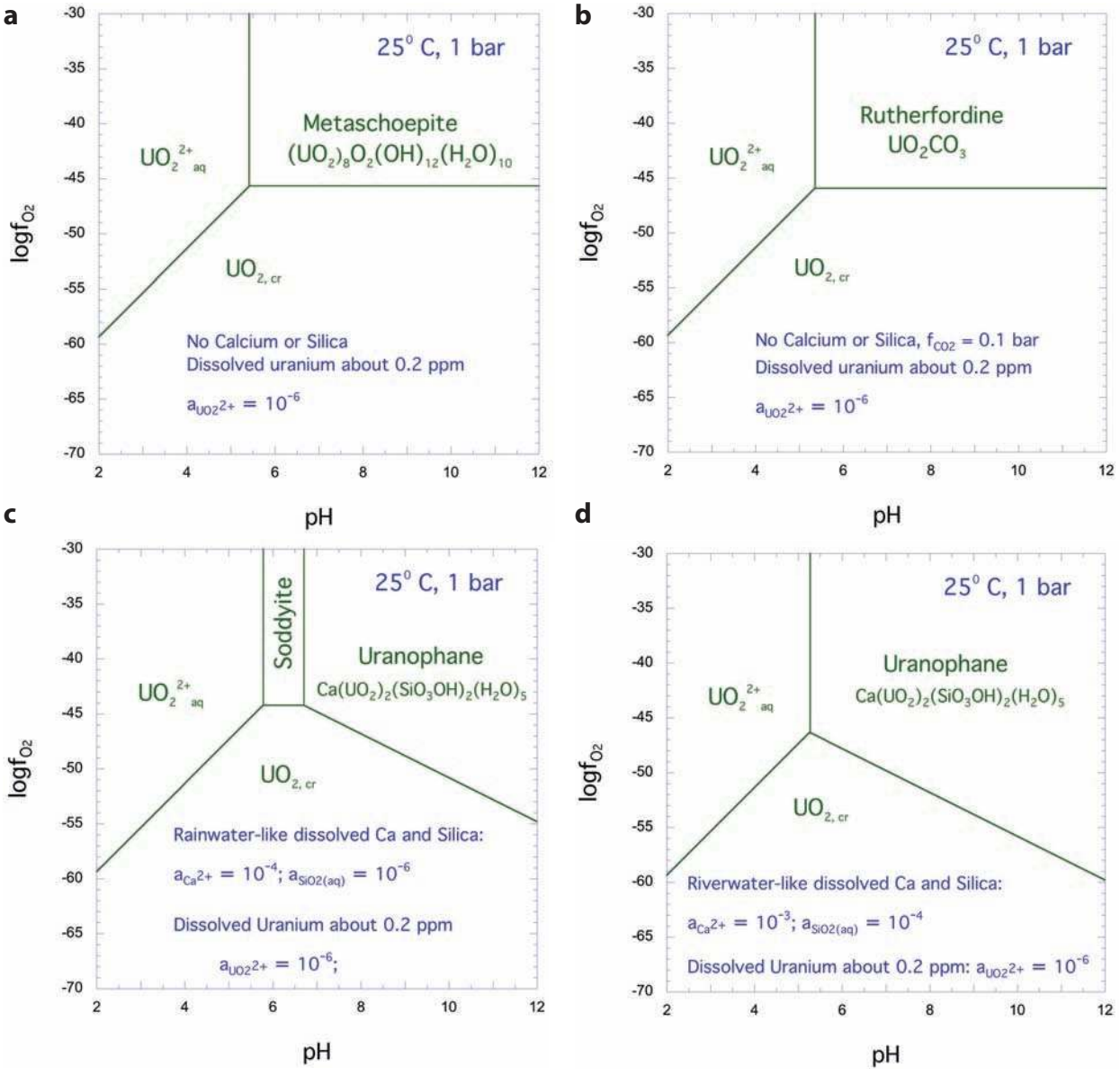

FIGURE 4. Calculated log f_{O_2}-pH diagrams illustrating the stability of uraninite ($UO_{2, cr}$) relative to a variety of uranyl minerals at 25 °C and 1 bar. The solubilities of the minerals are expressed relative to an aqueous activity for $(UO_2)^{2+}_{(aq)}$ of 10^{-6}. Aqueous complexing of $(UO_2)^{2+}_{(aq)}$ (for example, with carbonate or phosphate) could significantly expand the field of $(UO_2)^{2+}_{(aq)}$ relative to the minerals. Calculations are based on data of Shock et al. (1997a, 1997b), Chen et al. (1999), and Finch and Murakami (1999).

The first of these alteration mechanisms occurs when uranium decays to lead. If U^{4+} decays to Pb^{2+}, then charge compensation is achieved primarily by U^{4+} oxidizing to U^{6+} (Frondel 1958). This process initially changes the composition of the uraninite from the ideal UO_2 fluorite-structure end-member to $[(U^{4+}_{1-x-z-v}U^{6+}_xM^{2+}_zv^{4-}_v)O_{2+x-z-2v}]$, where v indicates metal site vacancies. The flexibility of the fluorite crystal structure allows UO_2 to accommodate these changes as U^{4+} is oxidized, up to a composition approximating $UO_{2.25}$.

An alternative auto-oxidation mechanism is suggested by the work of Kramers et al. (2009), who argue that radiogenic lead in zircon is tetravalent. They point to several lines of evidence, including anomalously slow Pb diffusion rates, incompatible Pb^{2+} crystal chemistry, and XANES spectra. This conclusion is further supported by the work of Utsunomiya et al. (2004), who observe that some Pb substitutes for Zr in the zircon structure. It is intriguing to speculate whether subsequent reduction of radiogenic Pb^{4+} to Pb^{2+} in zircon or other U-bearing mineral might be accompanied by auto-oxidation of U^{4+} to U^{6+} post-radioactive decay, and thus uranium oxidation is not necessarily synchronous with decay.

A second alteration mechanism becomes significant at uraninite compositions more oxidized than $UO_{2.25}$, where the fluorite structure cannot accommodate the added U^{6+}. The excess U^{6+} may become aqueous uranyl $(U^{6+}O_2)^{2+}$ ions, which promote uranyl oxyhydroxide minerals that initially can form an alteration rind

on the uraninite (Fig. 6), even in the absence of an oxic environment. These earliest U^{6+} uraninite alteration minerals include the mixed-valence mineral ianthinite $[U_2^{4+}(U^{6+}O_2)_4O_6 \cdot 9H_2O]$, as well as schoepite $[(UO_2)_8O_2(OH)_{12} \cdot 12H_2O]$, and becquerelite $[Ca(UO_2)_6O_4(OH)_6 \cdot 8H_2O]$ (Finch and Ewing 1992b; Finch 1994; Finch and Murakami 1999).

A third uraninite alteration mechanism occurs in conjunction with the radiogenic production of Pb^{2+}, which is incompatible at concentrations greater than a few percent in the uraninite structure (Janeczek and Ewing 1995). If sulfur activity is high enough, then galena (PbS) will form and the volume of uraninite may decrease without any U^{6+} going into solution (Finch and Murakami 1999). In the absence of sufficient S, however, uraninite may exsolve into Pb-rich and Pb-poor domains. In addition, lead production coupled with auto-oxidation may lead to the formation of several new Pb-uranyl secondary minerals (Fig. 7), including vandendriesscheite $[Pb_{1.6}(UO_2)_{10}O_6(OH)_{11} \cdot 11H_2O]$, fourmarierite $[Pb_{1-x}O_{3-2x}(UO_2)_4(OH)_{4+2x} \cdot 4H_2O]$, and kasolite $[Pb(UO_2)SiO_4 \cdot H_2O]$, which replaces sklowdowskite as Pb content increases (Finch and Ewing 1992a; Isobe et al. 1992). This process of Pb-U-mineral formation may be enhanced by preferential removal of U^{6+} compared with Pb^{2+} at mineral surfaces by groundwaters, which results in rinds of Pb-rich minerals. Thus Pb-rich uranyl oxy-hydroxides may form without high concentrations of dissolved Pb (Frondel 1958; Finch and Ewing 1992a, 1992b; Finch and Murakami 1999).

In some rare instances a fourth alteration mechanism occurs. It is possible to form uranyl peroxides, such as studtite $[(UO_2)_2O_2(H_2O)_2 \cdot 2H_2O]$ and metastudtite $[(UO_2)O_2(H_2O)_2]$, due to the radiolysis of thin films of water and the formation of hydrogen peroxide at the surface (Kubatko et al. 2003).

A fifth alteration mechanism that imposes a unique influence on all uranium and thorium minerals stems from long-term accumulation of damage caused by α-decay events. The aperiodic structure that results from radiation damage is known as the metamict state (Hoffmann 1987). Zircon often suffers from radiation damage caused by even low concentrations of U and Th; hence, zircon has figured most prominently in studies of the metamict state (Ewing et al. 2003; Utsunomiya et al. 2007). The widespread distribution of zircon in the continental crust, its tendency to concentrate trace elements (particularly lanthanides and actinides), its use in age-dating, and its resistance to chemical and physical degradation have made zircon the most important accessory mineral in geologic studies—providing one of the most precise views of Earth's evolution from its earliest period (Harley and Kelly 2007).

Although the concentrations of uranium and thorium in zircon are generally less than about 5000 ppm (Deer et al. 1997), some zircon crystals are of great age (the oldest dated zircon grains are >4 Ga) and, thus, have calculated doses of $>10^{19}$ α-decay events per gram, well beyond the dose required for the radiation-induced transformation to the metamict state. In an α-decay event, the α-particle dissipates most of its energy (4.0 to 6.0 MeV for actinides) by ionization processes over a range of 10 to 20 μm, but undergoes enough elastic collisions along its path to produce several hundred isolated atomic displacements. The largest number of displacements occurs near the end of the α-particle trajectory. The more massive, but lower energy, α-recoil (70 keV ^{234}Th-recoil from decay of ^{238}U) dissipates nearly all of its energy in elastic collisions over only 30 to 40 nm, transferring enough kinetic energy to cause ~2000

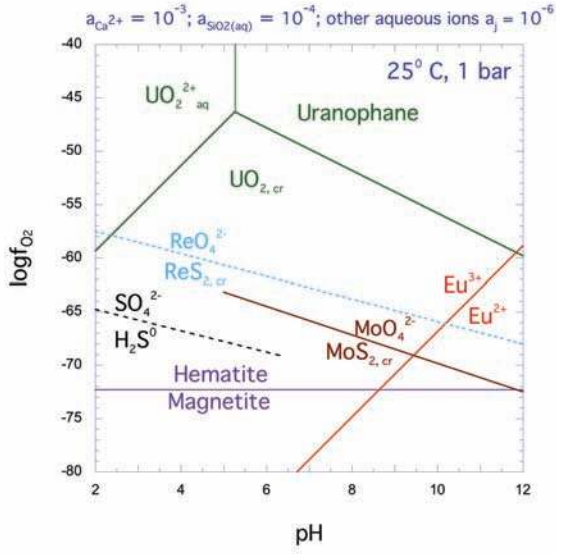

FIGURE 5. The Archean environment was highly reducing, characterized by the predominance of $H_2S \approx SO_4^{2-}$, $Fe^{2+} \gg Fe^{3+}$, $Mo^{4+} \gg Mo^{6+}$, and $Re^{4+} \gg Re^{7+}$, as well as the presence of atmospheric H_2 and the transportation of detrital ferroan carbonates (Rasmussen and Buick 1999; Catling and Claire 2005; Sverjensky and Hazen, in prep.). All of these redox couples imply an effective oxygen fugacity at intermediate pH significantly lower than the U^{4+}/U^{6+} equilibrium. We conclude that few of the more than 200 known uranyl minerals could have formed prior to the Great Oxidation Event. Calculations are based on data in Mills (1974) and Shock et al. (1997a, 1997b).

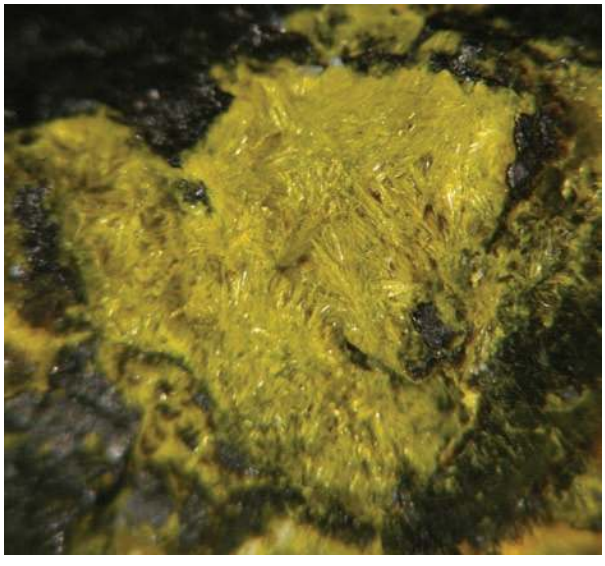

FIGURE 6. Uranyl oxyhydroxide minerals commonly form an alteration rind on the uraninite. Here, yellow schoepite $[(UO_2)_8O_2(OH)_{12} \cdot 12H_2O]$ forms pseudomorphs after acicular ianthinite $[U_2^{4+}(U^{6+}O_2)_4O_6 \cdot 9H_2O]$ crystals (from Shinkolobwe, Congo). Photo courtesy of Robert Lauf. Field of view is 6 mm wide.

Figure 7. Auto-oxidation leads to the formation of Pb-uranyl secondary minerals. Here reddish orange fourmarierite [$Pb_{1-x}O_{3-2x}(UO_2)_4(OH)_{4+2x}\cdot 4H_2O$] and bright orange vandendriesscheite [$Pb_{1.6}(UO_2)_{10}O_6(OH)_{11}\cdot 11H_2O$], along with pale yellow rutherfordine [$(UO_2)(CO_3)$], form a crust of secondary minerals on massive primary uraninite (UO_2) from Shinkolobwe, Congo. Photo courtesy of Robert Lauf. Specimen is 5 cm wide.

atomic displacements according to calculations (Weber 1993; Devanathan et al. 2006). This process creates a cascade of atomic collisions in which the total energy can be as much as 1 eV per atom, and whose structure and evolution can only be modeled by computer simulations. The cascade duration is extremely short ($<10^{-12}$ s), after which displacements by elastic interactions cease and the cascade gradually loses energy as it cools to ambient temperature, typically "quenching" in picoseconds. During this cooling phase, relaxation and diffusion reduce the number of displaced atoms in the cascade and the final damage state consists of a small low-density core surrounded by a halo of interstitials (Devanathan and Weber 2008).

The ^{238}U and ^{232}Th decay chains have eight and six α-decay events, respectively. Because of the large number of atomic displacements during an α-decay event, the accumulation and overlap of the individual cascades, as well as the presence of still crystalline but highly strained domains, has a profound effect on the structure and properties of the damaged solid. Zircon may experience a dramatic decrease in density (17%), a decrease in birefringence until isotropic, a decrease in the elastic moduli (69%), a decrease in hardness (40%), an increase in fracture toughness, and an increase in dissolution rate of one to two orders of magnitude. Over extended time, the final damage-induced microstructure is both time and temperature dependent because of annealing and recrystallization of damaged and strained domains. Radiation damage effects also occur in other minerals, including apatite, in which the effect of radiation damage on helium loss is the fundamental basis of thermochronology (Shuster et al. 2006; Shuster and Farley 2009).

In contrast, uraninite is quite resistant to α-decay damage, as a consequence of its relatively rapid annealing kinetics (Stout et al. 1988; Janeczek and Ewing 1991). Nevertheless, the damage process in uraninite may result in a redistribution of key elements, such as Pb, and facilitate the formation of coffinite, $USiO_4$, through interaction with Si-bearing groundwater (Deditius et al. 2009). An intriguing additional mode of alteration is the formation of bubbles in U minerals due to radiogenic He (Finch 1994; Roudil et al. 2008).

Thorium mineral evolution

The natural abundance of thorium is ~3× greater than that of uranium, whereas the size, valence, and crystal-chemical properties of Th^{4+} are nearly identical to those of U^{4+}. One might, therefore, expect Th minerals to exceed U minerals in abundance. Tetravalent Th and U minerals do typically form solid solutions and most of the ~30 known minerals that incorporate significant Th either incorporate U as an essential element, or have isostructural U species (http://rruff.info/ima/). Thus, for example, thorianite (ThO_2) is isostructural with uraninite, thorite ($ThSiO_4$) is isostructural with coffinite, and thorutite [$(Th,U,Ca)Ti_2(O,OH)_6$] is isostructural with brannerite. The most important economic deposits of thorium occur in the monazite [$(REE)PO_4$] structure type, which includes huttonite [$(Th,U)SiO_4$] and cheralite [$(Ce,Ca,Th,U)(P,Si)O_4$], whereas both Th and U are essential elements in some rare minerals of the pyrochlore, polycrase, rhabdophane, columbite, and iraqite groups (Staatz 1974; Stuart et al. 1983; Rasmussen and Glover 1994; Hiçsönmez and Eral 2001; Mordberg 2004; Zaccarini et al. 2004).

However, despite the congruence of initial Th and U mineralization, thorium differs significantly from uranium in at least three respects that limit its relative mineral diversity. First, Th only occurs in the tetravalent state, and therefore it does not have an analog of the uranyl ion and does not form isomorphs of the numerous uranyl minerals. Second, the half-life of ^{232}Th (the only significant natural isotope of Th) is ~14 billion years, so thorium minerals have not been subject to the same extensive degree of radiation damage and chemical alteration (including Pb production and auto-oxidation) as U minerals. Third, as discussed above, Th^{4+} is extremely insoluble in aqueous solutions, except as Th-fluoride complexes, so it does not enter aqueous solutions with U^{6+} or when U^{4+} is complexed by chloride or carbonate. Consequently, hydrothermal processes involving chloride- and/or carbonate-rich fluids can provide an effective means to separate U^{4+} from Th^{4+}. Indeed, the ratio of U to Th, for example in uraninite deposits, provides an important indicator of the extent of prior hydrothermal processes (Langmuir 1978; Keppler and Wylie 1990). Thus, whereas primary uraninite formed from granitic residual fluids typically has Th/U > 0.01 and may exceed 0.10, uraninite formed by aqueous transport of aqueous U^{6+} complexes into reducing environments typically has significantly lower Th/U (Frondel 1958; Plant et al. 1999).

Phase III—Uranium mineralization after the Great Oxidation Event (2.2 Ga)

The rise of atmospheric oxygen at about 2.2 Ga had major effects on uranium mobility and concentration in both the subsurface and near-surface Earth environments. Large, low-grade, detrital uraninite deposits no longer formed stably in fluvial environments. However, large high-grade hydrothermal uraninite deposits appeared in the subsurface, containing uraninite very low in thorium as compared with uraninite deposited prior to the

Great Oxidation Event. Thus, the modes of accumulation and compositions of uraninite were drastically affected by the GOE. In the near-surface environment, weathering conditions involved molecular O_2 for the first time, resulting in oxidative weathering of pyrite and other sulfide minerals and the formation of uranyl-bearing aqueous solutions. The latter could result from oxidative weathering of pre-existing reduced uranium minerals and by leaching of uranium from low-grade sources. As a consequence, ~200 uranyl minerals were able to form for the first time.

Formation of hydrothermal uraninite from uranyl-bearing solutions

The oldest hydrothermal uraninite deposits are the unconformity- and vein-type ore bodies in the Alligator Rivers region of the Northern Territory of Australia (1.6 Ga), the Athabasca region of Saskatchewan Canada (1.8 Ga), and the Franceville Basin of southeastern Gabon (2.0 Ga). Because of their size and age, these deposits have been intensively investigated and much is known about the conditions under which they formed (Kyser and Hiatt 2003; Derome et al. 2003a, 2003b; Jefferson et al. 2007). The special physicochemical conditions of formation appear to be an indirect consequence of the GOE. The Franceville deposits are also of interest because of their unique importance preserving a record of natural nuclear reactor conditions (see below).

Unconformity-type uraninite deposits are spatially related to an unconformity between the Early Proterozoic basement and overlying Middle Proterozoic sandstone. The disposition of the ore is controlled by faulting and fracturing of the basement and the sandstone (Komninou and Sverjensky 1996; Jefferson et al. 2007). Ore is located exclusively within the basement rocks in the Australian deposits, whereas in many of the Canadian deposits it is partially or completely located within the overlying sandstone. Hydrothermal alteration, fluid inclusion, reaction path, and reactive-transport modeling studies of the deposits indicate that free convection of saline uranium-bearing groundwaters at temperatures of 150 to 300 °C was followed by precipitation of uraninite associated with reduction by graphite, methane, and/or ferrous iron (Raffensperger and Garven 1995a, 1995b; Komninou and Sverjensky 1995a, 1995b, 1996; Jefferson et al. 2007). Thermodynamic, electron microprobe, and electron microscope studies of the chlorites in the Alligator River unconformity-type deposits suggest that uranium may have been transported predominantly as $(UO_2)^{2+}$-chloride complexes at f_{O_2} conditions substantially above those defined by the magnetite-hematite assemblage (Wilde and Wall 1987; Komninou and Sverjensky 1995b; Cuney et al. 2003; Jefferson et al. 2007). Such conditions are unusual for hydrothermal fluids in sedimentary basinal settings (Sverjensky 1984, 1987; Komninou and Sverjensky 1996) and raise the question of how these f_{O_2} conditions were achieved.

The physicochemical conditions achieved by potential ore-forming hydrothermal solutions are strongly influenced by the geologic formations traversed in the subsurface in groundwater flow systems. Interaction of potential ore-forming hydrothermal solutions with evaporitic units in the subsurface has long been suggested as a mechanism for the acquisition of both high salinity and increases in f_{O_2}. Reaction with calcium sulfate-bearing evaporites is a means of adding sulfate to a hydrothermal fluid, which increases the $(SO_4)^{2-}/HS^-$ ratio of the fluid, and which in turn increases the f_{O_2} (at constant pH). Note, however, that sulfate-rich fluids are not required for this mechanism, but only that the ratio of sulfate to sulfide be higher than in most other hydrothermal systems. Such reactions can elevate the oxidation state of a hydrothermal fluid substantially (Sverjensky 1987), and may have been responsible for the relatively high oxidation state of the ore-forming fluids in the unconformity-type uranium deposits (Komninou and Sverjensky 1995b, 1996). This suggestion provides a link to the GOE. It is likely that calcium sulfate-bearing evaporites did not become part of the geologic record until after the GOE (Anbar and Knoll 2002). If such rocks are essential to the generation of potential uranyl-bearing hydrothermal ore-forming fluids, then it helps to explain the appearance of the unconformity-type uranium ore deposits in the geologic record after the GOE.

Natural nuclear fission reactors

One of the unique aspects of uranium is that the ^{235}U isotope is fissile and a critical mass in the right configuration can lead to nuclear chain reactions that consume the ^{235}U. In 1972, uranium ore from Gabon was discovered to be deficient in ^{235}U, and it was quickly established that this anomaly was due to the occurrence of sustained fission reactions in the uranium deposits of the Franceville Basin. A total of 14 natural fission reactors have been identified in the Oklo-Okélobondo deposit, as well as another at Bangombé ~25 km to the southeast (Janeczek 1999; Jensen and Ewing 2001). These natural reactors are typically lens-shaped bodies, ~10 m in diameter and 10 to 50 cm thick.

The geologic occurrence of natural fission reactions has been the subject of intense study, initially because it represents such an unusual event in Earth's history (Naudet 1991; Gauthier-Lafaye et al. 1996), and more recently because of its potential implications for the geologic disposal of fissile material in used nuclear fuels (Oversby 1996). Four main conditions are required to sustain these nuclear reactions. First, the proportion of ^{235}U must be high. Two billion years ago the proportion of ^{235}U was 3.67% in uranium, as compared with 0.72% today. Due to the shorter half-life of ^{235}U vs. ^{238}U (7.04×10^8 vs. 4.47×10^9 years), the ratio of ^{235}U to ^{238}U has decreased steadily over geologic time. Two billion years ago the isotopic composition of uranium was not very different from that of a typical reactor fuel enriched in ^{235}U for modern light-water reactors.

A second requirement for a natural fission reactor is that neutron-absorbing elements, such as the rare-earth elements, must be in low concentrations in the reactor zone. Third, the environment must be rich in light elements, such as H and C, because the high-energy neutrons from fission (2×10^6 eV) must be slowed by ballistic interactions, "thermalized" (to 0.025 eV), to increase the probability of fission of ^{235}U. And fourth, the uranium ore must reach a sufficient concentration in the correct geometry in order sustain the nuclear reactions. Calculations have shown that criticality at Oklo was easily achieved in a 2 m thick layer of ore with 10 to 16 wt% U and a pore volume of 15 to 18 vol% for the moderating water (Naudet 1991).

During criticality, the Gabon reactors reached temperatures of 400 to 500 °C, creating small geothermal systems that, by the dissolution and reprecipitation of silicates, were able to further

increase the uranium concentration in the reactor zone. Because of the rather specific neutronic requirements for the occurrence of natural reactors, they provide a unique record of the Great Oxidation Event (Gauthier-Lafaye and Weber 2003; Horie et al. 2008). The very rich ores of the Oklo and Okélobondo deposits could not have accumulated until uranium could be transported hydrothermally as $(UO_2)^{2+}$-chloride complexes at estimated temperatures of 130 to 150 °C. According to Janeczek (1999), these oxidized saline fluids leached uranium from detrital uraniferous thorite grains in a basal fluvial conglomerate of 2.14 Ga age and then deposited uraninite after encountering reduced hydrocarbon-bearing fluids in the overlying sandstones. The richest ore subsequently became a nuclear reactor zone.

As with other Paleoproterozoic uraninite deposits, the mobilization of uranium may have required the availability of $CaSO_4$-bearing evaporitic units whose formation was only possible after the GOE. Thus, it was not until approximately two billion years ago that uranium could be mobilized as the more soluble $(UO_2)^{2+}$ species, the concentration of oxygen having risen rapidly due to photosynthetic microorganisms. Subsequent to this time, it was not possible to have sustained nuclear fission reactions because of the decreasing concentrations of ^{235}U.

It is also possible that biology played other indirect roles in the precipitation of the Oklo ore bodies. The uranium may have been reduced and concentrated when the oxidized solutions came into contact with bio-organic material in tectonic traps. Note that all of these conditions are also consistent with the direct microbially mediated precipitation of reduced U at a redox front (Lovely et al. 1991; Fayek et al. 2005). Hence, the natural reactors in the uranium deposits of the Franceville Basin, Gabon, record a unique combination of the geochemical, biological, and neutronic properties of uranium. In contrast, the only natural isotope of thorium, ^{232}Th, which cannot be concentrated by redox reactions, is also not fissile. The thorium fuel cycle is based on "breeding" ^{233}U by neutron capture reactions on ^{232}Th; hence, there are no natural Th-based reactors.

Formation of uranyl minerals in the near-surface environment

We postulate that the majority of the ~200 known uranyl minerals, which are secondary or tertiary oxidized and hydrated alteration products of other uranyl minerals, are unlikely to have appeared prior to the Great Oxidation Event (~2.2 Ga). This episode of dramatic atmospheric change was the result of oxygenic photosynthesis by cyanobacteria. Thus, we propose that perhaps 80 to 90% of Earth's uranium mineral species formed as an indirect consequence of microbial activity after 2.2 Ga.

It is likely that on a non-living planet, photo-oxidation coupled with uraninite auto-oxidation will lead gradually to an ever diversifying repertoire of uranyl mineral species. As many as two dozen uranium minerals, including several "first-generation" uranyl minerals such as ianthinite, schoepite, and becquerelite, can form under anoxic atmospheric conditions (e.g., Fig. 4a). Nevertheless, most of Earth's U minerals are oxidized weathering products (e.g., Korzeb et al. 1997): alteration and replacement of first-generation uranyl oxyhydroxides leads to soddyite $[(UO_2)_8O_2(OH)_{12}\cdot 12H_2O]$, weeksite $[(K,Ba)_{1-2}(UO_2)_2(Si_5O_{13})\cdot H_2O]$, curite $\{Pb_{3+x}[(UO_2)_4O_{4+x}(OH)_{3-x}]_2\cdot 2H_2O\}$, sklowdowskite $[Mg(UO_2)_2(SiO_3OH)_2\cdot 6H_2O]$, uranophane $[Ca(UO_2)_2(SiO_3OH)_2\cdot 5H_2O]$, and other minerals (Fig. 8). Uraninite alteration commonly leads to the complex mixed-phase material "gummite" (Fig. 9), which consists of a fine-grained mixture of soddyite, curite, kasolite, uranophane, boltwoodite $[KUO_2(SiO_3OH)\cdot H_2O]$, and clarkeite $[(Na,Ca,Pb)(UO_2)O(OH)\cdot nH_2O]$ (Frondel 1956; Foord et al. 1997).

Uranyl minerals can also dehydrate irreversibly (Čejka 1999), leading to highly soluble phases that may reprecipitate as other uranyl minerals. For example, the uranium carbonate

Figure 8. Lemon yellow schoepite $[(UO_2)_8O_2(OH)_{12}\cdot 12H_2O]$, amber becquerelite $[Ca(UO_2)_6O_4(OH)_6\cdot 8H_2O]$, and orange curite $\{Pb_{3+x}[(UO_2)_4O_{4+x}(OH)_{3-x}]_2\cdot 2H_2O\}$ represent progressive alteration of black uraninite (UO_2) under oxidizing conditions (specimen from Shinkolobwe, Congo). Photo courtesy of Robert Lauf. Specimen is 2 cm in its longest dimension.

Figure 9. Dendritic uraninite mostly altered to "gummite," which is a mixture of several uranyl minerals, including soddyite, curite, kasolite, uranophane, boltwoodite, and clarkeite (Frondel 1956; Foord et al. 1997). This pegmatitic specimen is from the Ruggles Mine, New Hampshire. Photo courtesy of Robert Lauf. Specimen is 5 cm wide.

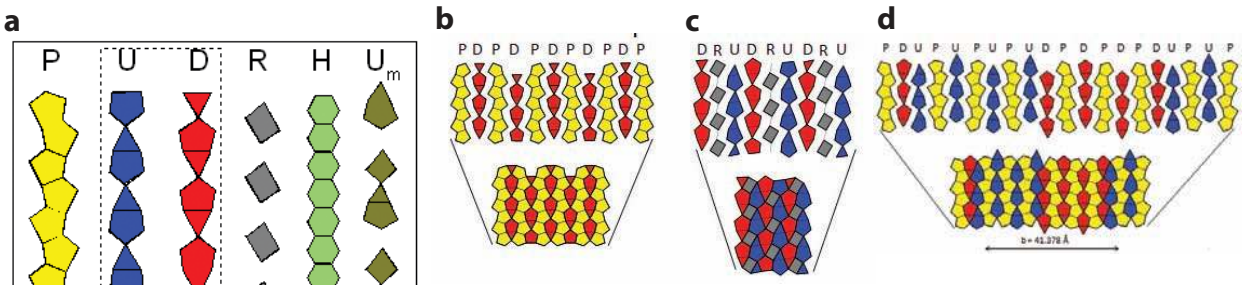

FIGURE 10. Four chain-types (Miller et al. 1996) found in uranyl minerals (**a**), combine to form dozens of different sheet topologies, including the α–U_3O_8 sheet (**b**), the β–U_3O_8 sheet (**c**), and the structural layer of vandendriesscheite [$Pb_{1.6}(UO_2)_{10}O_6(OH)_{11}\cdot 11H_2O$] (courtesy of Peter Burns).

rutherfordine [$(UO_2)(CO_3)$] will precipitate readily from low-pH, carbonate-rich solutions. Curiously, ionizing radiation from the decay of U can cause some of these uranyl minerals to decompose and form nano-crystals of UO_2, which may be again oxidized to form U^{6+}-phases (Utsunomiya et al. 2005).

The role of pentavalent uranium

The discovery of seven-coordinated U^{5+} in the mineral wyartite [$CaU^{5+}(UO_2)_2(CO_3)O_4(OH)\cdot 7H_2O$] by Burns and Finch (1999a), coupled with electrochemical studies of U^{5+}-mediated uraninite dissolution (Goldik et al. 2004; Santos et al. 2006; Broczkowski et al. 2007) and the spectroscopic identification of U^{5+} at the surface of altered uraninite (Sunder et al. 1996; Santos et al. 2004; Schindler et al. 2009), suggest a potentially important role for uranium's intermediate valence state. Pentavalent uranium is commonly associated with the corrosive alteration of UO_2 SIMFUEL over a wide range of temperature (Broczkowski et al. 2007), pH (Santos et al. 2006), and solutes (Goldik et al. 2004). Indeed, without the transitions $U^{4+} \rightarrow U^{5+}$ and $U^{5+} \rightarrow U^{6+}$, the rates for uraninite oxidation and uranyl reduction would be much lower, and perhaps kinetically inhibited (Schindler et al. 2009; Schindler, personal communication). Thus, while U^{5+} plays a minor role volumetrically, it may be essential to the mobility of uranium and thus the formation of many uranium minerals.

Crystal chemistry and paragenesis of uranyl minerals

U^{6+} almost always adopts the near-linear $(U^{6+}O_2)^{2+}$ uranyl ion configuration (Burns et al. 1997). In U^{6+} minerals, the linear uranyl molecule is surrounded by either four, five, or six O atoms that form an equatorial ring around the U atom, perpendicular to the length of the uranyl ion (Burns 1999). The $<U^{6+}\text{-}O_{uranyl}>$ bond length is ~1.8 Å, whereas the bond lengths to the equatorial O atoms, $<U^{6+}\text{-}O_{\phi}>$, are in a range 2.1 to 2.4 Å (Burns 2005). These equatorial O atoms are under-bonded; hence, uranium coordination polyhedra usually polymerize by sharing edges, and this distinctive behavior leads to the large number of sheet structures that are characteristic of uranyl minerals (Burns 1999, 2005). The sheets of the uranyl minerals can be described as consisting of four chain-types (Miller et al. 1996), and the hundreds of sheet topologies can be understood as different combinations of these chains (Fig. 10).

Remarkably, this understanding of the topology of the structural units of uranyl minerals can be elegantly combined with a bond-valence theory and used to predict their occurrence from derived compositional-activity diagrams (Schindler and Hawthorne 2004). The uranyl structures are analyzed in terms of the types of chains in each sheet (Fig. 10) and the interstitial complexes that consist of metals and the different roles of water (Schindler and Hawthorne 2008). The stability of the U^{6+} phases can be predicted as a function of pH and $\log[M^{2+}]$ activity diagrams from the ratio of molar proportions of the metal (MO) + H_2O to the molar proportion of UO_3 in the structural unit (Fig. 11). This ratio, $[(MO) + (H_2O)]/(UO_3)$, depends on the topology of the chains that make up the sheets, as illustrated on the right side of Figure 11.

In solution, uranyl ions easily form complexes, mainly by bonding of the equatorial O atoms. Principal among them are uranyl carbonates that are quite soluble and mobile. The high solubility, and thus mobility, of the uranyl ion is the single most important difference in the geochemical behavior of U vs. Th. Hence, the ~0.003 ppm concentration of U in seawater is significantly greater than the ~0.000009 ppm concentration of Th (Emsley 1991; Table 2).

A variety of uranyl complexes are able to form in near-surface

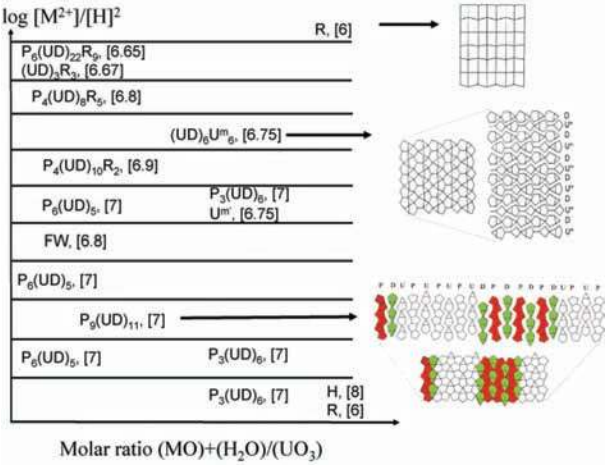

FIGURE 11. The activity-composition diagram $\log[M^{2+}]/[H^+]^2$ vs. the molar ratio $[(MO) + (H_2O)]/(UO_3)$. FW indicates a framework structure. The average coordination of U is given in square brackets. The chain-stacking sequences of the corresponding anion topologies are graphically represented to the right. Three examples are shown: the anion topology of synthetic $Pb^{2+}[(UO_2)O_2]$ (top), curite (center), and vandendriesscheite (bottom) (from Schindler and Hawthorne 2004).

oxidizing zones, where changes in solution chemistry can lead to the precipitation of a host of distinctive U^{6+} minerals (Finch and Murakami 1999; Lauf 2008). In the absence of fluorine, $(U^{6+}O_2)^{2+}$ forms hydrated aqueous complexes at pH < 5 and hydroxide complexes at pH > 5. In U-rich solutions, polymeric $(UO_2)_x$ often forms extended hydroxide complexes. Such solutions are poised to form a variety of hydrated uranyl minerals.

In carbonated waters at higher pH, uranyl ions form carbonate complexes, which may be the most common groundwater species. Uranyl carbonates precipitate when evaporation is high or fugacity of CO_2 is greater than atmospheric values (Garrels and Christ 1959; Finch 1997). Finch and Murakami (1999) list more than 30 uranyl carbonate minerals. Some of these minerals are found only as weathering products of mine tailings, whereas others occur as alteration products of previously formed uranyl carbonates (Fig. 12).

In low-pH sulfate-bearing waters, uranyl sulfate complexes are observed. Uranyl sulfate minerals (~20 known species) only form where sulfides are being oxidized to produce aqueous SO_4 ions, coupled with evaporation (Fig. 13). Similarly, uranyl selenides and tellurides (nine known species) occur where Se- and Te-bearing sulfides are oxidized to produce $(Se^{4+}O_3)^{2-}$ or Te aqueous ions (Finch and Murakami 1999).

The uranyl silicates uranophane and β-uranophane are the most common U^{6+} minerals (Fig. 14), though almost 20 other uranyl silicates are known, as tabulated by Finch and Murakami (1999). They observe that uranosilite $[(UO_2)Si_7O_{15}]$ forms only in "highly oxidizing environments," whereas oursinite $[Co(UO_2)_2(SiO_3OH)_2 \cdot 6H_2O]$ forms from oxidation of primary Co and Ni sulfides.

By far the most diverse U^{6+} minerals are the uranyl phosphates and arsenates, with more than 70 known species (e.g., Huminicki and Hawthorne 2002; Locock and Burns 2003; Locock et al. 2005). Uranyl arsenates precipitate when preexisting arsenides or As-bearing sulfides are oxidized, thus releasing aqueous AsO_4. Finch and Murakami (1999) describe an alteration sequence of uranyl oxy-hydroxides, to chernikovite $[(H_3O)(UO_2)(PO_4) \cdot 3H_2O]$, to other uranyl phosphates, which are observed as the last stage of uranyl mineral evolution, and they form in the most oxidized zones (Fig. 15). This sequence requires acidic conditions (under which apatite is more soluble).

uraninite dissolution → uranyl oxyhydroxides →
uranyl silicates, carbonates and Pb-enriched phases →
continued replacement by uranyl oxyhydroxides →
uranyl phosphates

Uranyl vanadates, tungstates, and molybdates (24 known species) are quite insoluble. The vanadates will precipitate anywhere

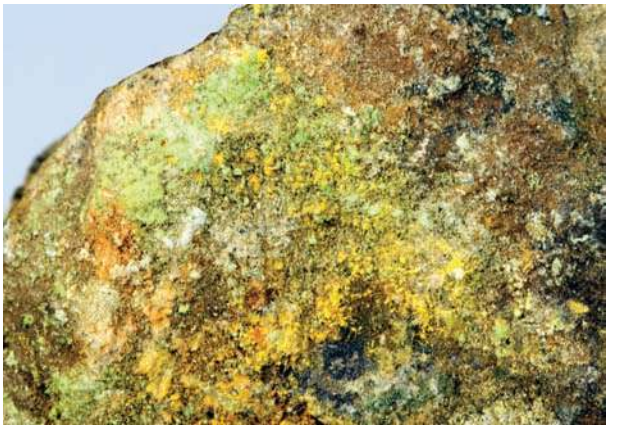

FIGURE 13. Uranyl sulfate minerals (~20 known species) only form where sulfides are being oxidized to produce aqueous SO_4 ions, coupled with evaporation. Here pale green johannite $[Cu(UO_2)_2(SO_4)_2(OH)_2 \cdot 8H_2O]$ occurs with yellow zippeite $[K_3(UO_2)_4(SO_4)_2O_3(OH) \cdot 3H_2O]$ in a specimen from Roughton Consols, Bodmin Moor, Cornwall, England. Photo courtesy of Robert Lauf. Field of view is 3 cm wide.

FIGURE 12. Many of the ~30 known uranyl carbonate species are found only as weathering products of mine tailings, while others occur as alteration products of previously formed uranyl carbonates. Here yellow kamotoite-(Y) $[Y_2O_4(UO_2)_4(CO_3)_3 \cdot 14H_2O]$ forms as small crystals on altered uraninite (UO_2). Photo courtesy of Robert Lauf. Field of view is 2.5 cm wide.

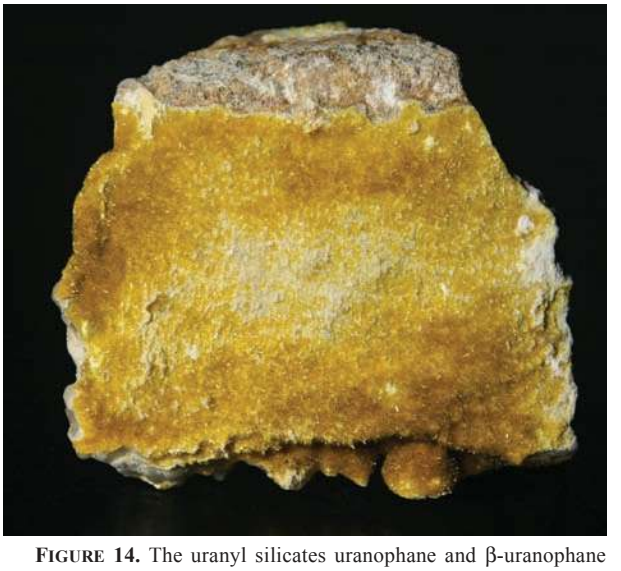

FIGURE 14. The uranyl silicates uranophane and β-uranophane $[Ca(UO_2)_2(SiO_3OH)_2 \cdot 5H_2O]$ are the most common U^{6+} minerals. Here β-uranophane needles coat a matrix surface (specimen from Rössing, Namibia). Photo courtesy of Robert Lauf. Specimen is ~10 cm wide.

reduced U and V minerals coexist and are undergoing oxidation, which produces aqueous U^{6+} and V^{5+}.

Uranyl minerals, which are structurally less robust than uraninite, are also subject to alteration through radiogenic decay. Finch et al. (1995, 1996) record that some uranyl minerals persist for hundreds of thousands to millions of years, but others, including highly soluble phases, are ephemeral, dissolving in rain or dehydrating under surface evaporation. Čejka (1999), who reviewed thermal decomposition of many uranyl minerals, records that dehydration occurs in one or more steps to 200 °C, with dehydroxylation up to 350 to 400 °C. U_3O_8 is found to be the thermal end product for several U minerals, though no polymorph of U_3O_8 has been identified as a mineral.

Phase IV—Uranium mineralization mediated by organics (0.4 Ga)

The rise of land plants and the resulting organic-rich terrestrial sediments ~400 million years ago led to widespread uranium mineralization in a variety of carbon-rich lithologies, including lignite, black shale, and sandstone-type ore deposits (Nash et al. 1981; Dahlkamp 1993; Finch 1996; Plant et al. 1999; McKay and Meiitis 2001; Lally and Bajwah 2006). Low-temperature, near-surface uranyl-bearing solutions precipitate uraninite and coffinite when U^{6+}-rich solutions contact zones rich in reduced organic materials, such as kerogen, or from H_2S produced by sulfate-reducing bacteria (Fig. 16). Indeed, the most important near-surface sink for U is reduction in anoxic sediments (Suzuki and Banfield 1999), including marine sediments and the organic-rich sediments of estuaries (Swarzenski et al. 2003). These examples of uraninite deposition since the Paleozoic Era are similar in chemical origins to those of much earlier graphite-mediated unconformity-type ore bodies. However, the evolution of a terrestrial biosphere dramatically altered the quantity and distribution of reduced organic matter available for uranium reduction.

Sandstone-type ore deposits, which hold a significant fraction of known uranium reserves in the United States and Australia, are controlled by the movement of groundwater through coarse-grained sandstones. The reduction of U^{6+} to U^{4+} occurs at sediment-water redox boundaries, where organic-rich anoxic sediments that include fragments of plants produce the distinctive curving shape of the roll front uranium deposits (Goldhaber et al. 1978; Nash et al. 1981; Klinkhammer and Palmer 1991; Cochran 1992). A sharp boundary separates a lighter-colored oxidized zone from the dark organic material mixed with uraninite (Fig.

Figure 15. An alteration sequence of uranyl oxy-hydroxides to uranyl phosphates is observed to be the last stage of uranyl mineral evolution. Autunite $[Ca(UO_2)_2(PO_4)_2 \cdot 10–12(H_2O)]$ and its many isomorphs are among the most common of the more than 40 species of uranyl phosphates. This specimen is from Luzy, France. Photo courtesy of Robert Lauf. Specimen is 7 cm wide; the largest autunite crystals are ~8 mm across.

Figure 16. Massive black coffinite (ideally $USiO_4$), with a yellow coating of the secondary uranyl sulfate zippeite $[K_3(UO_2)_4(SO_4)_2O_3(OH) \cdot 3H_2O]$, formed in the sediment-hosted Grants mineral belt, Section 35 Mine, Jurassic Morrison Formation, New Mexico. Photo courtesy of Robert Lauf. Specimen is 7 cm wide; individual masses of zippeite are up to ~1 mm.

Figure 17. Dark-colored U^{4+} minerals, including uraninite and coffinite, form roll front type ore deposits when they come into contact with reducing, organic material in terrestrial sediments. These important economic resources formed only during the past 400 million years, since the rise of land plants. Photo courtesy of Andrew Alden. This outcrop was featured as stop 10, 2007 GSA Field Guide 428. The field of view is ~3 m across.

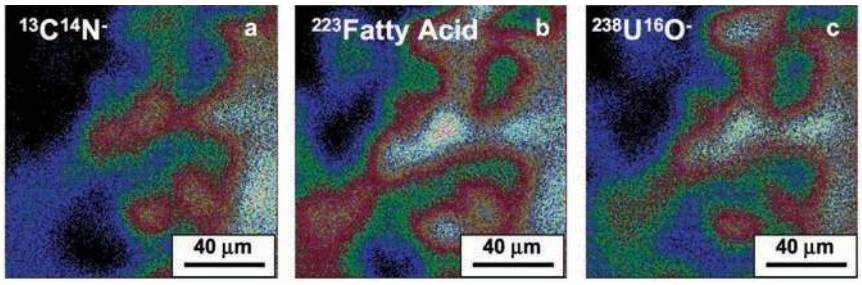

◀**FIGURE 18.** Data of Fayek et al. (2005) reveal that some microbes couple enzymatic metabolic acetate oxidation to the reduction of aqueous uranyl cations $(U^{6+}O_2)^{2+}$ to uraninite. These micro-SIMS images of (**a**) $^{13}C^{14}N$ molecules and (**b**) fatty acids that mark the location of *Geobacter* biofilms match the location of $^{238}U^{16}O$ (**c**). These images thus show that where there are no bacteria, there is also no uranium oxide. Courtesy of Mostafa Fayek.

17). These boundaries move over time and form linear trends that can extend laterally for many kilometers.

Uranium can also be removed from solution without forming discrete phases through interaction with a variety of minerals. For example, uranium is commonly found in marine phosphorites as a trace element replacing Ca in apatite. Typical concentrations are less than 1000 ppm (Dahlkamp 1993; Plant et al. 1999), though some phosphorite deposits of great extent represent some of the largest known uranium reserves (Cathcart 1989).

Uranium in solution as $(UO_2)^{2+}$ and its complexes also adsorb onto fine-grained minerals such as Fe-oxide-hydroxides and silica and onto sediments (Hsi and Langmuir 1985; Waite et al. 1994; Kohler et al. 1966; Davis et al. 2004; Curtis et al. 2006) as well as co-precipitating with calcite (Reeder et al. 2001; Kelly et al. 2003). Experiments in these systems have demonstrated that at low pH uranium adsorption is minimal, $(UO_2)^{2+}$ behaves as a cation, and its adsorption increases with pH at values of about 4 to 6. At pH values of about 7 to 10, uranium is strongly adsorbed in the absence of carbonate complexes, but becomes desorbed in the presence of carbonate complexes when it behaves as an anionic complex of carbonate. Consequently, there is typically a maximum at near neutral pH values for the adsorption of uranium in CO_2-bearing solutions. Bentonite (a smectite clay) not only adsorbs U^{6+}, but it also catalyzes the reduction to insoluble U^{4+} by interaction with adsorbed organic matter (Giaquinta et al. 1997). This adsorption is also highly pH dependent (Schmeide et al. 2000; Lenhart and Honeyman 1999). Biological activity can also trigger the reaction of uranyl oxyhydroxides with sulfate- or carbonate-bearing groundwater to produce uranium oxysalt minerals, such as rutherfordine.

MICROBIAL MEDIATION OF URANIUM MINERALS

In addition to their formation of an oxygen-rich atmosphere, microbes are known to mediate uranium mineral formation in several other ways. For example, microbes can undergo metabolism-dependent metal uptake by precipitation of insoluble uranyl phosphates; i.e., *Citrobacter* sp. precipitates autunite $[Ca(UO_2)_2(PO_4)_2 \cdot 10–12(H_2O)]$. Some microbes, including *Geobacter*, *Desulfovibrio*, and *Shewanella*, are known to couple enzymatic metabolic acetate oxidation to the reduction of aqueous uranyl cations $(U^{6+}O_2)^{2+}$ to uraninite (Lovely et al. 1991; Fayek et al. 2005; Long 2008; Sharp et al. 2008; Fig. 18). The biogenic precipitation of uraninite nanoparticles is also being pursued as a means to remediate U^{6+}-contaminated groundwater (Wu et al. 2007; Yabusaki et al. 2007; Bargar et al. 2008).

In contrast, Beller (2005) has reported the direct microbial oxidation of uraninite to soluble uranyl ions, coupled to nitrate reduction in *Thiobacillus denitrificans*. In addition, Chinni et al. (2008) have documented indirect uranium oxidation by *Bacillus* sp. These microbes oxidize Mn^{2+} to Mn^{4+} oxides, which in turn chemically oxidize U^{4+} in UO_2 to U^{6+}, thereby mobilizing uranium. These examples of direct microbially induced oxidation or reduction of uranium are consistent with other diverse microbial metabolic redox strategies (Nealson 1997).

Even in the absence of U-altering metabolic activity, microbes can passively concentrate U through metabolism-independent intracellular U uptake. In this process, U passively migrates through the cell membrane and binds to organic molecules in the cell (Suzuki and Banfield 1999). Microbes can thus desolubilize uranium and aid in the remediation of U-contaminated groundwaters (Campbell et al. 2008).

DISCUSSION AND CONCLUSIONS

Uranium minerals exemplify the principles of mineral evolution (Hazen et al. 2008). The first phase, from ~4.5 to 3.5 Ga, involved successive concentrations of uranium and thorium from their initial uniform trace distribution into magmatic-related fluids from which U-Th-bearing zircons and the first U^{4+} and Th^{4+} minerals, uraninite, thorite, and coffinite, precipitated in the crust. The second period, from ~3.5 to 2.2 Ga, saw the formation of large low-grade concentrations of Th-rich detrital uraninite in the Witwatersrand-type quartz-pebble conglomerates deposited in a highly anoxic near-surface environment. Abiotic alteration of uraninite and coffinite, including auto-oxidation caused by radioactive decay and the formation of helium from alpha particles, may have resulted in the formation of a limited suite of uranyl oxide-hydroxides.

Earth's third phase of uranium mineral evolution, during which most known U minerals first precipitated from reactions of soluble uranyl $(U^{6+}O_2)^{2+}$ ions, followed the GOE at ~2.2 Ga and thus was mediated indirectly by biological activity. The low-Th uraninite deposited during this phase is represented in unconformity- and vein-type U deposits. During this phase, most uranyl minerals were able to form for the first time in the O_2-bearing near-surface environment through weathering processes.

The most recent phase of uranium mineral evolution coincided with the rise of land plants and formation of organic-rich terrestrial and shallow marine sediments. Sediment-hosted uranium ore bodies formed at redox fronts, where organic matter reduced low-temperature, near-surface, uranyl-rich waters and led to the precipitation of uraninite and coffinite. Thus, the modes of accumulation and even the compositions of uraninite as well

as the common oxidation states of U (4+ vs. 6+) are a sensitive indicator of global redox conditions.

In contrast, the behavior of thorium, which has only a single oxidation state (4+) that has a very low solubility in the absence of aqueous F-complexes, cannot reflect changing redox conditions. Geochemical concentration of Th relative to U at high temperatures is therefore limited to special magmatic-related environments where U^{4+} is preferentially removed by chloride or carbonate complexes and at low temperatures to mineral surface reactions.

Throughout Earth's history three principal mechanisms have driven the evolution of Earth's near-surface uranium mineralogy. The first mechanism included physical and chemical processes, such as planetary differentiation, partial melting of silicate rocks, and leaching by hydrothermal fluids, which separated U (and to a lesser extent Th) from other elements. These gradual processes of concentration transformed an initially homogeneous chondritic element distribution with U < 10 ppb into localized reservoirs of uranium, enriched by a factor of 10^6, in which uraninite was initially precipitated.

The second mechanism of uranium mineral evolution was the subjection of varying U-bearing compositions to an increased range of intensive variables, including temperature, pressure, and the activities of volatiles such as H_2O, CO_2, and O_2. Of special importance to uranium minerals are the gradual processes of auto-oxidation and radiation damage that result from radiogenic decay to Pb.

The third and arguably most dramatic driving force for uranium mineral evolution has been the influence of living organisms. Life creates and sustains local- to global-scale compositional gradients that promote reaction pathways that lead to new minerals. In particular, as many as 200 of the known uranium minerals occur as a consequence of microbially induced atmospheric oxidation, which is the single most important cause for mineralogical diversification at or near Earth's surface. In addition, microbes mediate the precipitation of uranium minerals through active metabolism and passive adsorption.

The extent of these three mechanisms will vary significantly on different terrestrial planets and moons. Without repeated cycles of fluid processing, uranium will never achieve local concentrations sufficient to precipitate uraninite. Thus, we postulate that no uranium or thorium minerals would have occurred on planetessimals in the early solar system, nor will they be found on volatile-poor bodies such as the Moon or Mercury. Indeed, if the large-scale hydrothermal activity associated with plate tectonics is required, then Mars and perhaps Venus will also be devoid of discrete U and Th mineral phases.

If, however, uraninite forms, then a sequence of additional uranium minerals must follow as a consequence of Pb production, auto-oxidation, and the formation of uranyl phases. Nevertheless, in the absence of microbial activity and an oxygenated atmosphere, most of the uranium minerals found on Earth today are unlikely to form. Uranium minerals may thus represent useful mineralogical targets in the search for life on other worlds.

Acknowledgments

We gratefully acknowledge the contributions of Robert Lauf, who provided original photographs of uranium minerals from his personal collection. We benefited from helpful discussions and constructive reviews from Associate Editor Peter Dahl, as well as from Gregory Dick, Mostafa Fayek, Robert Finch, Russell Hemley, Stephen Kesler, Robert Lauf, Michael Schindler, Brian Skinner, and an anonymous reviewer. R.M.H. and D.A.S. acknowledge support from the National Science Foundation, the NASA Astrobiology Institute, and the Carnegie Institution of Washington. R.C.E. acknowledges support from the Office of Basic Energy Sciences of the Department of Energy (DE-FG02-06ER15783).

References cited

Adam, Z. (2007) Actinides and life's origins. Astrobiology, 7, 852–872.

Anbar, A.D. and Knoll, A.H. (2002) Proterozoic ocean chemistry and evolution: a bioinorganic bridge? Science, 297, 1137–1142.

Anbar, A.D., Duan, Y., Lyons, T.W., Arnold, G.L., Kendall, B., Creaser, R.A., Kaufman, A.J., Gordon, G.W., Scott, C., Garvin, J., and Buick, R. (2007) A whiff of oxygen before the Great Oxidation Event. Science, 317, 1903–1906.

Bargar, J.R., Bernier-Latmani, R., Giammar, D.E., and Tebo, B.M. (2008) Biogenic uraninite nanoparticles and their importance for uranium remediation. Elements, 4, 407–412.

Beller, H.R. (2005) Anaerobic, nitrate-dependent oxidation of U(IV) oxide minerals by the chemolithoautotrophic bacterium *Thiobacillus denitrificans*. Applied and Environmental Microbiology, 71, 2170–2174.

Bertine, K.K., Chan, L.H., and Turekian, K.K. (1970) Uranium determinations in deep-sea sediments and natural waters using fission tracks. Geochimica et Comsochimica Acta, 34, 641–648.

Blundy, J. and Wood, B. (2003) Mineral-melt partitioning of uranium, thorium and their daughters. In B. Bourdon, G.M. Henderson, C.C. Lundstrom, and S.P. Turner, Eds., Uranium-series Geochemistry, 52, p. 59–124. Reviews in Mineralogy and Geochemistry, Mineralogical Society of America, Chantilly, Virginia.

Bourdon, B. and Sims, K.W.W. (2003) U-series constraints on intraplate basaltic magmatism. In B. Bourdon, G.M. Henderson, C.C. Lundstrom, and S.P. Turner, Eds., Uranium-series Geochemistry, 52, p. 215–254. Reviews in Mineralogy and Geochemistry, Mineralogical Society of America, Chantilly, Virginia.

Bourdon, B., Henderson, G.M., Lundstrom, C.C., and Turner, S.P., Eds. (2003) Uranium-series Geochemistry, 52, 656 p. Reviews in Mineralogy and Geochemistry, Mineralogical Society of America, Chantilly, Virginia.

Broczkowski, M.E., Noel, J.J., and Shoesmith, D.W. (2007) The influence of temperature on the anodic oxidation/dissolution of uranium dioxide. Electrochimica Acta, 52, 7386–7395.

Burns, P.C. (1999) The crystal chemistry of uranium. In P.C. Burns and R. Finch, Eds., Uranium: Mineralogy, Geochemistry and the Environment, 38, p. 23–90. Reviews in Mineralogy and Geochemistry, Mineralogical Society of America, Chantilly, Virginia.

——— (2005) U^{6+} minerals and inorganic compounds: Insights into an expanded structural hierarchy of crystal structures. Canadian Mineralogist, 43, 1839–1894.

Burns, P.C. and Finch, R.J. (1999a) Wyartite: crystallographic evidence for the first pentavalent-uranium mineral. American Mineralogist, 84, 1456–1460.

——— (Editors) (1999b) Uranium: Mineralogy, Geochemistry and the Environment, 38, 677 p. Reviews in Mineralogy and Geochemistry, Mineralogical Society of America, Chantilly, Virginia.

Burns, P.C., Ewing, R.C., and Hawthorne, F.C. (1997) The crystal chemistry of hexavalent uranium: Polyhedron geometries, bond-valence parameters, and polymerization of polyhedra. Canadian Mineralogist, 35, 1551–1570.

Campbell, K.M., Qafoku, N.P., Kukkadapu, R., Williams, K.H., Lesher, E., Figueroa, L., Peacock, A., Wilkins, M.J., Davis, J.A., Icenhower, J., and Long, P.E. (2008) Characterizing the extent and role of natural subsurface bioreduction in a uranium-contaminated aquifer [abstract]. Geochimica et Cosmochimica Acta, 72, A133.

Cathcart, J.B. (1989) The phosphate deposits of Florida with a note on the deposits in Georgia and South Carolina, U.S.A. In A.J.G. Notholt, R.P. Sheldon, and D.F. Davidson, Eds., Phosphate Deposits of the World, Volume 2: Phosphate Rock Resources, p. 62–70. Cambridge University Press, U.K.

Catling, D.C. and Claire, M.W. (2005) How Earth's atmosphere evolved to an oxic state: A status report. Earth and Planetary Science Letters, 237, 1–20.

Čejka, J. (1999) Infrared spectroscopy and thermal analysis of the uranyl minerals. In P.C. Burns and R. Finch, Eds., Uranium: Mineralogy, Geochemistry and the Environment, 38, p. 521–622. Reviews in Mineralogy and Geochemistry, Mineralogical Society of America, Chantilly, Virginia.

Chen, F., Ewing, R.C., and Clark, S.B. (1999) The Gibbs free energies and enthalpies of formation of U^{6+} phases: An empirical method of prediction. American Mineralogist, 84, 650–654.

Chen, J.H. and Wasserberg, G.J. (1986) The U-Th-Pb systematics in hot springs on the East Pacific Rise at 21°N and Guayamas Basin. Geochimica et Cosmochimica Acta, 50, 2467–2479.

Chinni, S., Anderson, C.R., Ulrich, K.-U., Giammar, D.E., and Tebo, B.M. (2008) Indirect UO_2 oxidation by Mn(II)-oxidizing spores of *Bacillus* sp. Strain SG-1 and the effect of U and Mn concentrations. Environmental Science and Technology, 42, 8709–8714.

Cochran, J.K. (1992) The oceanic chemistry of uranium—and thorium—series

nuclides. In M. Ivanovich and R.S. Harmon, Eds., Uranium-series Disequilibrium: Applications to Earth, Marine, and Environmental Sciences, p. 334–395. Clarendon Press, Oxford.
Crisp, J.A. (1984) Rates of magma emplacement and volcanic output. Journal of Volcanological and Geothermal Research, 20, 177–211.
Cuney, M. and Kyser, K., Eds. (2009) Recent and Not-so-recent Developments in Uranium Deposits and Implications for Exploration, 39, 257 p. Short Course Series, Mineralogical Association of Canada, Quebec, Canada.
Cuney, M., Brouand, M., Cathelineau, M., Derome, D., Freiberger, R., Hecht, L., Kister, P., Lobaev, V., Lorilleux, G., Peiffert, C., and Bastoul, A.M. (2003) What parameters control the high grade, large tonnage of the Proterozoic unconformity related uranium deposits? In M. Cuney, Ed., Uranium Geochemistry 2003, International Conference, April 13–16 2003, Proceedings, p. 123–126. Unité Mixte de Recherche CNRS 7566 G2R, Université Henri Poincaré, Nancy, France.
Curtis, G.P., Davis, J.A., and Naftz, D.L. (2006) Simulation of reactive transport of uranium(VI) in groundwater with variable chemical conditions. Water Resources Research, 42, W04404, DOI: 10.1029/2005WR003979.
Dahlkamp, F.J. (1993) Uranium Ore Deposits, 460 p. Springer-Verlag, Berlin.
Davis, J.A., Meece, D.E., Kohler, M., and Curtis, G.P. (2004) Approaches to surface complexation modeling of Uranium(VI) adsorption on aquifer sediments. Geochimica et Cosmochimica Acta, 68, 3621–3641.
Deditius, A.P., Utsunomiya, S., Wall, M.A., Pointeau, V., and Ewing, R.C. (2009) Crystal chemistry and radiation-induced amorphization of P-coffinite from the natural fission reactor at Bangombé, Gabon. American Mineralogist, 94, 827–836.
Deer, W.A., Howie, R.A., and Zussman, J. (1997) Rock-forming Minerals, Volume 1A Orthosilicates, second edition, 919 p. The Geological Society, London.
Derome, D., Cuney, M., Cathelineau, M., Fabre, C., Dubessy, J., Bruneton, P., and Hubert, A. (2003a) A detailed fluid inclusion study in silicified breccias from the Kombolgie sandstones (Northern Territory, Australia): inferences for the genesis of middle-Proterozoic unconformity-type uranium deposits. Journal of Geochemical Exploration, 80, 259–275.
Derome, D., Cathelineau, M., Lhomme, T., and Curley, M. (2003b) Fluid inclusion evidence of the differential migration of H_2 and O_2 in the McArthur River unconformity-type uranium deposit (Saskatchewan, Canada). Possible role on post-ore modifications of the host rocks. Journal of Geochemical Exploration, 78–79, 525–530.
Devanathan, R. and Weber, W.J. (2008) Dynamic annealing of defects in irradiate zirconia-based ceramics. Journal of Materials Research, 23, 593–597.
Devanathan, R., Corrales, L.R., Weber, W.J., Chartier, A., and Meis, C. (2006) Molecular dynamics simulation of energetic uranium recoil damage in zircon. Molecular Simulation, 32, 1069–1077.
Eisenbud, M. and Gesell, T. (1997) Environmental Radioactivity, 656 p. Academic Press, New York.
Emsley, J. (1991) The Elements, second edition, 251 p. Oxford University Press, New York.
England, G.L., Rasmussen, B., Krapez, B., and Groves, D.L. (2002) Paleoenvironmental significance of rounded pyrite in siliciclastic sequences of the Late Archean Witwatersrand Basin: Oxygen-deficient atmosphere or hydrothermal alteration. Sedimentology, 49, 1133–1136.
Ewing, R.C. (1999) Radioactivity in the 20th century. In P.C. Burns and R. Finch, Eds., Uranium: Mineralogy, Geochemistry and the Environment, 38, p. 1–21. Reviews in Mineralogy and Geochemistry, Mineralogical Society of America, Chantilly, Virginia.
Ewing, R.C., Meldrum, A., Wang, L.M., Weber, W.J., and Corrales, L.R. (2003) Radiation effects in zircon. In J.M. Hanchar and P.W.O. Hoskin, Eds., Zircon, 53, p. 387–425. Reviews in Mineralogy and Geochemistry, Mineralogical Society of America, Chantilly, Virginia.
Fareeduddin, J.A.S. (1990) Significance of the occurrence of detrital pyrite and uraninite on the Kalaspura conglomerate, Karnataka. Indian Minerals, 44, 335–340.
Fayek, M. and Kyser, T.K. (1997) Characterization of multiple fluid-flow events and rare-earth-element mobility associated with formation of unconformity-type uranium deposits in the Athabasca basin, Saskatchewan. Canadian Mineralogist, 35, 627–658.
Fayek, M.J., Utsunomiya, S., Pfiffner, S.M., Anovitz, L.M., White, D.C., Riciputi, L.R., Ewing, R.C., and Stadermann, F.J. (2005) Nanoscale chemical and isotopic characterization of *Geobacter sulfurreducens* surfaces and bio-precipitated uranium minerals. Canadian Mineralogist, 43, 1631–1641.
Finch, R.J. (1994) Paragenesis and crystal chemistry of uranyl oxide hydrates, 257 p. Ph.D. thesis, University of New Mexico, Albuquerque.
——— (1997) Thermodynamic stabilities of U(VI) minerals: Estimated and observed relationships. Materials Research Society Symposium Proceedings, 465, 1185–1192.
Finch, R.J. and Ewing, R.C. (1992a) The corrosion of uraninite under oxidizing conditions. Journal of Nuclear Materials, 190, 133–156.
——— (1992b) Alteration of uranyl oxide hydrates in Si-rich groundwaters: Implications for uranium solubility. Materials Research Society Symposium Proceedings, 257, 465–472.
Finch, R.J. and Murakami, T. (1999) Systematics and paragenesis of uranium minerals. In P.C. Burns and R. Finch, Eds., Uranium: Mineralogy, Geochemistry and the Environment, 38, p. 91–180. Reviews in Mineralogy and Geochemistry, Mineralogical Society of America, Chantilly, Virginia.
Finch, R.J., Suksi, J., Rasilainen, K., and Ewing, R.C. (1995) Long-term stability of becquerelite. Materials Research Society Symposium Proceedings, 353, 647–652.
——— (1996) Uranium series ages of secondary minerals with applications to the long-term storage of spent nuclear fuel. Materials Research Society Symposium Proceedings, 412, 823–830.
Finch, W.I. (1996) Uranium provinces of North America—their definition, distribution, and models. United States Geological Survey Bulletin, 2141.
Foord, E.E., Korzeb, S.L., Lichte, F.E., and Fitzpatrick, J.J. (1997) Additional studies on mixed uranyl oxide-hydroxide hydrate alteration products of uraninite from the Palermo and Ruggles granite pegmatites, Grafton County, New Hampshire. Canadian Mineralogist, 35, 145–151.
Frimmel, H.E. (2005) Archaean atmospheric evolution: evidence from the Witwatersrand gold fields, South Africa. Earth-Science Reviews, 70, 1–46.
Frimmel, H.E. and Minter, W.E.L. (2002) Recent developments concerning the geological history and genesis of the Witwatersrand gold deposits, South Africa. In R.J. Goldfarb and R.L. Nielsen, Eds., Integrated Methods for Discovery: Global Exploration in the Twenty-First Century, 9, p. 17–45. Society of Economic Geologists Special Publication, Littleton, Colorado.
Frondel, C. (1956) The mineralogical composition of gummite. American Mineralogist, 41, 539–568.
——— (1958) Systematic mineralogy of uranium and thorium. United States Geological Survey Bulletin, 1064, 400 p.
Garrels, R.M. and Christ, C.L. (1959) Behavior of uranium minerals during oxidation. In R.M. Garrels and E.S. Larsen, Eds., Geochemistry and Mineralogy of the Colorado Plateau Uranium Ores. United States Geological Survey Professional Paper, 320, p. 81–89.
Gauthier-Lafaye, F. and Weber, F. (2003) Natural nuclear fission reactors: Time constraints for occurrence, and their relation to uranium and manganese deposits and to the evolution of the atmosphere. Precambrian Research, 120, 81–100.
Gauthier-Lafaye, F., Holliger, P., and Blanc, P.-L. (1996) Natural fission reactors in the Franceville basin, Gabon: a review of the conditions and results of a "critical event" in a geological system. Geochimica et Cosmochimica Acta, 60, 4831–4852.
Giaquinta, D.M., Soderholm, L., Yuchs, S.E., and Wassermann, S.R. (1997) The speciation of uranium in a smectite clay: Evidence for catalysed uranyl reduction. Radiochimica Acta, 76, 113–121.
Goldhaber, M.B., Reynold, R.L., and Rye, R.O. (1978) Origin of the south Texas roll type uranium deposit: II. Sulfide petrology and sulfur isotope studies. Economic Geology, 73, 1690–1705.
Goldik, J.S., Nesbitt, H.W., Noel, J.J., and Shoesmith, D.W. (2004) Surface electrochemistry of UO_2 in dilute alkaline hydrogen peroxide solutions. Electrochimica Acta, 49, 1699–1709.
Gorman-Lewis, D., Mazeina, L., Fein, J., Szymanowski, J., Burns, P.C., and Navrotsky, A. (2007) Thermodynamic properties of soddyite from solubility and calorimetry measurements. Journal of Chemical Thermodynamics, 39, 568–575.
Grandstaff, D.E. (1980) Origin of uraniferous conglomerates at Elliot Lake, Canada, and Witwatersrand, South Africa: Implications for oxygen in the Precambrian atmosphere. Precambrian Research, 13, 1–26.
Grenthe, I., Fuger, J., Konings, R., Lemire, R., Muler, A., Nguyen-Trung, C., and Wanner, H. (1992) Chemical Thermodynamics of Uranium, 715 p. Elsevier, Amsterdam.
Guillaumont, R., Fanghänel, T., Fuger, J., Grenthe, I., Neck, V., Palmer, D., and Rand, M. (2003) Update on the Chemical Thermodynamics of Uranium, Neptunium, Plutonium, Americium, and Technetium, 919 p. Elsevier, Amsterdam.
Harley, S.L. and Kelly, N.M. (2007) Zircon—tiny but timely. Elements, 3, 13–18.
Hazen, R.M. (2005) Genesis: The Scientific Quest for Life's Origins, 339 p. Joseph Henry Press, Washington, D.C.
Hazen, R.M., Papineau, D., Bleeker, W., Downs, R.T., Ferry, J.M., McCoy, T.J., Sverjensky, D.A., and Yang, H. (2008) Mineral evolution. American Mineralogist, 93, 1693–1720.
Hemingway, B.S. (1982) Thermodynamic properties of selected uranium compounds at 298.15 K and 1 bar and at higher temperatures: Preliminary models for the origin of coffinite deposits. United States Geological Survey Open-File Report 82-619.
Hiçsönmez, U. and Eral, M. (2001) Use of extraction chromatography for thorium purification from Eskisehir-Beylikahir thorium-REEs ore deposit. Radiochimica Acta, 89, 805–809.
Hoffmann, R. (1987) The Metamict State (Contemporary Poetry Series), 104 p. University Press of Florida, Gainesville.
Holland, H.D. (1984) The Chemical Evolution of the Atmosphere and Oceans, 588 p. Princeton University Press, New Jersey.

——— (1994) Early proterozoic atmospheric change. In S. Begtson, Ed., Early Life on Earth: Nobel Symposium 84, p. 237–244. Columbia University Press, New York.
Holmes, A. (1911) The association of lead with uranium in rock-minerals and its application to the measurement of geologic time. Proceedings of the Royal Society, Series A, 85, 248–256.
Horie, K., Hidaka, H., and Gauthier-Lafaye, F. (2008) Timing of the atmospheric oxygen evolution: Uranium transport in the Franceville series at Oklo, Gabon [abstract]. Geochimica et Cosmochimica Acta, 72, A390.
Hsi, C.D. and Langmuir, D. (1985) Adsorption of uranyl onto ferric hydroxides: Application of the surface complexation site-binding model. Geochimica et Cosmochimica Acta, 49, 1931–1941.
Huminicki, D.M.C. and Hawthorne, F.C. (2002) The crystal chemistry of the phosphate minerals. In M.L. Kohn, J. Rakovan, and J.M. Hughes, Eds., Phosphates: Geochemical, Geobiological, and Materials Importance, 48, p. 123–253. Reviews in Mineralogy and Geochemistry, Mineralogical Society of America, Chantilly, Virginia.
Isobe, H., Murakami, T., and Ewing, R.C. (1992) Alteration of uranium minerals in the Koongarra deposit, Australia: Unweathered zone. Journal of Nuclear Materials, 190, 174–187.
Janeczek, J. (1999) Mineralogy and geochemistry of natural fission reactors in Gabon. In P.C. Burns and R. Finch, Eds., Uranium: Mineralogy, Geochemistry and the Environment, 38, p. 321–392. Reviews in Mineralogy and Geochemistry, Mineralogical Society of America, Chantilly, Virginia.
Janeczek, J. and Ewing, R.C. (1991) X-ray powder diffraction study of annealed uraninite. Journal of Nuclear Materials, 185, 66–77.
——— (1995) Mechanisms of lead release from uraninite in the natural fission reactors in Gabon. Geochimica et Cosmochimica Acta, 59, 1917–1931.
Jefferson, C.W., Thomas, D.J., Gandhi, S.S., Ramaekers, P., Delaney, G., Brisbin, D., Cutts, C., Quirt, D., Portella, P., and Olson, R.A. (2007) Unconformity-associated uranium deposits of the Athabasca Basin, Saskatchewan and Alberta. In W.D. Goodfellow, Ed., Mineral Deposits of Canada: A Synthesis of Major Deposit Types, District Metallogeny, the Evolution of Geological Provinces, and Exploration Methods, 5, p. 273–305. Geological Association of Canada, Mineral Deposits Division, Special Publication, St. Johns.
Jensen, K.A. and Ewing, R.C. (2001) The Okélobondo natural fission reactor, southeast Gabon: Geology, mineralogy, and retardation of nuclear-reaction products. Geological Society of America Bulletin, 113, 32–62.
Kelly, S.D., Newville, M.G., Cheng, L., Kemner, K.M., Sutton, S.R., Fenter, P., Sturchio, N.C., and Spötl, C. (2003) Uranyl incorporation in natural calcite. Environmental Science and Technology, 37, 1284–1287.
Keppler, H. and Wyllie, P.J. (1990) Role of fluids in transport and fractionation of uranium and thorium in magmatic provinces. Nature, 348, 531–533.
Klinkhammer, G.P. and Palmer, M.R. (1991) Uranium in the oceans: Where it goes and why. Geochimica et Cosmochimica Acta, 55, 1799–1806.
Kohler, M., Curtis, G.P., Kent, D.B., and Davis, J.A. (1996) Experimental investigation and modeling of uranium (VI) transport under variable chemical conditions. Water Resources Research, 32, 3539–3551.
Komninou, A. and Sverjensky, D.A. (1995a) Pre-ore hydrothermal alteration in an unconformity-type uranium deposit. Contributions to Mineralogy and Petrology, 121, 99–114.
——— (1995b) Hydrothermal alteration and ore-forming fluid chemistry in an unconformity-type uranium deposit. Geochimica et Cosmochimica Acta, 59, 2709–2723.
——— (1996) Geochemical modeling of the formation of an unconformity-type uranium deposit. Economic Geology, 91, 590–606.
Korzeb, S.L., Foord, E.E., and Lichte, F.E. (1997) The chemical evolution and paragenesis of uranium minerals from the Ruggles and Palermo granitic pegmatites, New Hampshire. Canadian Mineralogist, 35, 135–144.
Kramers, J., Frei, R., Newville, M., Kober, B., and Villa, I. (2009) On the valency state of radiogenic lead in zircon and its consequences. Chemical Geology, 261, 4–11.
Kubatko, K.H., Helean, K.B., Navrotsky, A., and Burns, P.C. (2003) Stability of peroxide-containing uranyl minerals. Science, 302, 1191–1193.
——— (2005) Thermodynamics of uranyl minerals: Enthalpies of formation of rutherfordine, UO_2CO_3, andersonite, $Na_2CaUO_2(CO_3)_3(H_2O)_5$, and grimselite, $K_3NaUO_2(CO_3)_3H_2O$. American Mineralogist, 90, 1284–1290.
——— (2006) Thermodynamics of uranyl minerals: Enthalpies of formation of uranyl oxide hydrates. American Mineralogist, 91, 658–666.
Kumar, P. and Srinivasan, R. (2002) Fertility of Late Archaean basement granite in the vicinity of U-mineralized Neoproterozoic Bhima basin, peninsular India. Current Science, 82, 571–576.
Kyser, K. and Hiatt, E.E. (2003) Fluids in sedimentary basins: an introduction. Journal of Geochemical Exploration, 80, 139–149.
Lally, J. and Bajwah, Z. (2006) Uranium Deposits of the NT. Northern Territory Geological Survey Reports, 20.
Langmuir, D. (1978) Uranium solution-mineral equilibria at low temperatures with applications to sedimentary ore deposits. Geochimica et Cosmochimica Acta, 42, 547–569.
Lauf, R. (2008) Introduction to Radioactive Minerals, 144 p. Schiffer Publishing, Atglen, Pennsylvania.
Lee, N., Sverjensky, D.A., and Hazen, R.M. (2008) Oxidation state during weathering on the early Earth [abstract]. Geochimica et Cosmochimica Acta, 72, A921.
Lenhart, J.J. and Honeyman, B.D. (1999) Uranium(VI) sorption to hematite in the presence of humic acid. Geochimica et Cosmochimica Acta, 63, 2891–2901.
Locock, A.J. and Burns, P.C. (2003) The structure of hugelite, an arsenate of the phosphuranylite group, and its relationship to dumontite. Mineralogical Magazine, 67, 1109–1120.
Locock, A.J., Burns, P.C., and Flynn, T.M. (2005) The role of water in the structures of synthetic hallimondite, $Pb_2[(UO_2)(AsO_4)_2](H_2O)_n$ and synthetic parsonsite, $Pb_2[(UO_2)(PO_4)_2](H_2O)_n$, $0 \le n \le 0.5$. American Mineralogist, 90, 240–246.
London, D. (2008) Pegmatites, 347 p. Mineralogical Association of Canada, Special Publication 10.
Long, P.E. (2008) Field-scale bioreduction of U(VI) to U(IV) in an alluvial aquifer: Evidence for microbially mediated precipitation of uranium under both natural and biostimulated conditions [abstract]. Geochimica et Cosmochimica Acta, 72, A560.
Lovely, D.R., Phillips, E.J.P., Gorby, Y.A., and Landa, E.R. (1991) Microbial reduction of uranium. Nature, 350, 413–416.
Lundstrom, C.C. (2003) Uranium-series disequilibria in mid-ocean ridge basalts: Observations and models of basalt genesis. In B. Bourdon, G.M. Henderson, C.C. Lundstrom, and S.P. Turner, Eds., Uranium-series Geochemistry, 52, p. 175–214. Reviews in Mineralogy and Geochemistry, Mineralogical Society of America, Chantilly, Virginia.
McKay, A.D. and Meiitis, Y. (2001) Australia's uranium resources, geology and development of deposits. AGSO-Geoscience Australia, Mineral Resources Report 1.
Miller, M.L., Finch, R.J., Burns, P.C., and Ewing, R.C. (1996) Description and classification of uranium oxide hydrate sheet anion topologies. Journal of Materials Research, 11, 3048–3056.
Mills, K.C. (1974) Thermodynamic Data for Inorganic Sulfides, Selenides and Tellurides, 845 p. Butterworths, London.
Miyake, Y., Sugimura, Y., and Yasujima, T. (1970) Thorium concentration and the activity ratios $^{230}Th/^{232}Th$ and $^{228}Th/^{232}Th$ in sea water in the Western North Pacific. Journal of the Oceanographical Society of Japan, 26, 130–136.
Moore, W.S. (1967) Amazon and Mississippi river concentration of uranium, thorium, and radium isotopes. Earth and Planetary Science Letters, 2, 231–234.
Mordberg, L.E. (2004) Thorium in crandallite-group minerals: an example from a Devonian bauxite deposit, Timan, Russia. Mineralogical Magazine, 68, 489–497.
Murphy, W.M. and Shock, E.L. (1999) Environmental aqueous geochemistry of actinides. In P.C. Burns and R. Finch, Eds., Uranium: Mineralogy, Geochemistry and the Environment, 38, p. 221–254. Reviews in Mineralogy and Geochemistry, Mineralogical Society of America, Chantilly, Virginia.
Nash, J.T., Granger, H.C., and Adams, S.S. (1981) Geology and concepts of genesis of important types of uranium deposits. Economic Geology, 75th Anniversary Volume, 63–116.
Naudet, R. (1991) Oklo: Des Réacteurs Nucléaires Fossiles, 695 p. Eyrolles, Paris.
Nealson, K.H. (1997) Sediment bacteia: Who's there, what are they doing, and what's new? Annual Review of Earth and Planetary Sciences, 25, 403–434.
Oversby, V.M. (1996) Criticality in a high level waste repository—A review of some important factors and an assessment of the lessons that can be learned from the Oklo Reactors. SKB Technical Report 96-07, 41 p.
Palme, H. and O'Neill, H.St.C. (2003) Cosmochemical estimates of mantle composition. In R.W. Carlson, Ed., The Mantle and Core, 2, p. 1–38. Elsevier-Pergamon, Amsterdam.
Plant, J.A., Simpson, P.R., Smith, B., and Windley, B.F. (1999) Uranium ore deposits—products of the radioactive Echo Bay U-Ni-Ag-Cu deposits, North West Territories, Canada. Economic Geology, 68, 635–656.
Prasad, N. and Roscoe, S.M. (1996) Evidence of anoxic to oxic atmosphere change during 2.45–2.22 Ga from lower and upper sub-Huronian paleosols, Canada. Catena, 27, 105–121.
Pretorius, D.A. (1981) Gold and uranium in quartz–pebble conglomerates. Economic Geology, 75th Anniversary Volume, 117–138.
Raffensperger, J.P. and Garven, G. (1995a) The formation of unconformity-type uranium ore deposits. 1. Coupled groundwater flow and heat transport modeling. American Journal of Science, 295, 581–636.
——— (1995b) The formation of unconformity-type uranium ore deposits. 2. Coupled hydrochemical modeling. American Journal of Science, 295, 639–696.
Rasmussen, B. and Buick, R. (1999) Redox state of the Archean atmosphere: Evidence from detrital minerals in ca. 3250–2750 sandstones from the Pilbara Craton, Australia. Geology, 27, 115–118.
Rasmussen, B. and Glover, J.E. (1994) Diagenesis of low-mobility elements (Ti, REEs, Th) and solid bitumen envelopes in Permian Kennedy Group sandstone, western Australia. Journal of Sedimentary Research, 64, 572–583.
Reeder, R.J., Nugent, M., Tait, C.D., Morris, D.E., Heald, S.M., Beck, K.M.,

Hess, W.P., and Lanzirotti, A. (2001) Coprecipitation of uranium(VI) with calcite: XAFS, micro-XAS, and luminescence characterization. Geochimica et Cosmochimica Acta, 65, 3491–3503.
Reiners, P.W., Ehlers, T.A., and Zeitler, P.K. (2005) Past, present, and future of thermochronology. In P.W. Reiners and T.A. Ehlers, Eds., Low-Temperature Thermochronology: Techniques, Interpretations, and Applications, 58, p. 1–18. Reviews in Mineralogy and Geochemistry, Mineralogical Society of America, Chantilly, Virginia.
Roudil, D., Bonhoure, J., Pik, R., Cuney, M., Jégou, C., and Gauthier-Lafaye, F. (2008) Diffusion of radiogenic helium in natural uranium oxides. Journal of Nuclear Materials, 378, 70–78.
Santos, B.G., Nesbitt, H.W., Noel, J.J., and Shoesmith, D.W. (2004) X-ray photoelectron spectroscopy study of anodically oxidized SIMFUEL surfaces. Electrochimica Acta, 49, 1863–1873.
Santos, B.G., Noel, J.J., and Shoesmith, D.W. (2006) The effect of pH on the anodic dissolution of SIMFUEL UO_2. Journal of Electroanalytical Chemistry, 586, 1–11.
Santschi, P.H. and Honeyman, B.D. (1989) Radionuclides in aquatic environments. Radiation Physics and Chemistry, 34, 213–240.
Schindler, M. and Hawthorne, F.C. (2004) A bond-valence approach to the uranyl-oxide hydroxy-hydrate minerals: Chemical composition and occurrence. Canadian Mineralogist, 42, 1601–1627.
——— (2008) The stereochemistry and chemical composition of interstitial complexes in uranyl-oxysalt minerals. Canadian Mineralogist, 46, 467–501.
Schindler, M., Hawthorne, F.C., Freund, M.S., and Burns, P.C. (2009) XPS spectra of uranyl minerals and synthetic uranyl compounds. I: The U 4f spectrum. Geochimica et Cosmochimica Acta, 73, 2471–2487.
Schmeide, K., Pompe, S., Bubner, M., Heise, K.H., Bernhard, G., and Nitsche, H. (2000) Uranium(VI) sorption onto phyllite and selected minerals in the presence of humic acid. Radiochimica Acta, 88, 723–728.
Sharp, J.O., Schofield, E., Junier, P., Veeramani, H., Suvorova, E., Bargar, J.R., and Bernier-Latmani, R. (2008) Systematic investigation of the product of microbial U(VI) reduction by different bacteria (abstract). Geochimica et Cosmochimica Acta, 72, A852.
Shock, E.L., Sassani, D.C., and Betz, H. (1997a) Uranium in geologic fluids: Estimates of standard partial molal properties, oxidation potentials, and hydrolysis constants at high temperatures and pressures. Geochimica et Cosmochimica Acta, 61, 4245–4266.
Shock, E.L., Sassani, D.C., Willis, M., and Sverjensky, D.A. (1997b) Inorganic species in geologic fluids: Correlations among standard molal thermodynamic properties of aqueous ions and hydroxide complexes. Geochimica et Cosmochimica Acta, 61, 907–950.
Shuster, D.L. and Farley, K.A. (2009) The influence of artificial radiation damage and thermal annealing on helium diffusion kinetics in apatite. Geochimica et Cosmochimica Acta, 73, 183–196.
Shuster, D.L., Flowers, R.M., and Farley, K.A. (2006) The influence of natural radiation damage on helium diffusion kinetics in apatite. Earth and Planetary Science Letters, 249, 148–161.
Sleep, N.H. (1990) Hotspots and mantle plumes: Some phenomenology. Journal of Geophysical Research, 95, 6715–6736.
Smits, G. (1989) (U,Th)-bearing silicates in reefs in the Witwatersrand, South Africa. Canadian Mineralogist, 27, 643–656.
Staatz, M.H. (1974) Thorium veins in the United States. Economic Geology, 69, 494–507.
Stout, P.J., Lumpkin, G.R., Ewing, R.C., and Eyal, Y. (1988) An annealing study of alpha-decay damage in natural UO_2 and ThO_2. Materials Research Society Symposium Proceedings, 112, 495–504.
Stuart, E.J., Bornhurst, T.J., Rose, W.I., and Noble, D.C. (1983) Distribution and mobility of uranium and thorium in the peralkaline Soldier Meadow Tuff, northwestern Nevada. Economic Geology, 78, 353–358.
Sunder, S., Cramer, J.J., and Miller, N.H. (1996) Geochemistry of the Cigar Lake uranium deposit: XPS studies. Radiochimica Acta, 74, 303–307.
Suzuki, Y. and Banfield, J.F. (1999) Geomicrobiology of uranium. In P.C. Burns and R. Finch, Eds., Uranium: Mineralogy, Geochemistry and the Environment, 38, p. 393–432. Reviews in Mineralogy, Mineralogical Society of America, Chantilly, Virginia.
Sverjensky, D.A. (1984) Oil-field brines as ore-forming solutions. Economic Geology, 79, 23–37.
——— (1987) The role of migrating oil-field brines in the formation of sediment-hosted Cu-rich deposits. Economic Geology, 82, 1130–1141.
Swarzenski, P.W., Porcelli, D., Andersson, P.S., and Smoak, J.M. (2003) The behavior of U- and Th-series nuclides in the estuarine environment. In B. Bourdon, G.M. Henderson, C.C. Lundstrom, and S.P. Turner, Eds., Uranium-series Geochemistry, 52, p. 577–606. Reviews in Mineralogy and Geochemistry, Mineralogical Society of America, Chantilly, Virginia.
Taylor, S.R. (1964) The abundance of chemical elements in the crust—a new table. Geochimica et Cosmochimica Acta, 28, 835–839.
Tolstikhin, I.N. and Kramers, J.D. (2008) The Evolution of Matter from the Big Bang to the Present Day, 521 p. Cambridge University Press, New York.
Turner, G., Harrison, T.M., Holland, G., Mojzsis, S.J., and Gilmor, J. (2004) Extinct ^{244}Pu in ancient zircons. Science, 306, 89–91.
Turner, S., Bourdon, B., and Gill, J. (2003) Insights into magma genesis at convergent margins from U-series isotopes. In B. Bourdon, G.M. Henderson, C.C. Lundstrom, and S.P. Turner, Eds., Uranium-series Geochemistry, 52, p. 255–316. Reviews in Mineralogy and Geochemistry, Mineralogical Society of America, Chantilly, Virginia.
Utsunomiya, S., Palenik, C.S., Valley, J.W., Cavosie, A.J., Wilde, S.A., and Ewing, R.C. (2004) Nanoscale occurrence of Pb in an Archean zircon. Geochimica et Cosmochimica Acta, 68, 4679–4686.
Utsunomiya, S., Ewing, R.C., and Wang, L.M. (2005) Radiation-induced decomposition of U(VI) phases to nanocrystals of UO_2. Earth and Planetary Science Letters, 240, 521–528.
Utsunomiya, S., Valley, J.W., Cavosie, A.J., Wilde, S.A., and Ewing, R.C. (2007) radiation damage and alteration of zircon from a 3.3 Ga porphyritic granite from Jack Hills, Western Australia. Chemical Geology, 236, 92–111.
Vochten, R. and Van Haverbeke, L. (1990) Transformation of schoepite into the uranyl oxide hydrates: Becquerelite, billietite, and wölsendorfite. Mineralogy and Petrology, 43, 65–72.
Wagner, G.A. and Van den Haute, P. (1992) Fission-Track Dating, 285 p. Kluwer Academic Publishers, Dordrecht.
Waite, T.D., Davis, J.A., Payne, T.E., Waychunas, G.A., and Xu, N. (1994) Uranium(VI) adsorption to ferrihydrite: Application of a surface complexation model. Geochimica et Cosmochimica Acta, 58, 5465–5478.
Weber, W.J. (1993) Alpha-decay-induced amorphization in complex silicate structures. Journal of the American Ceramic Society, 76, 1729–1738.
Wilde, A.R. and Wall, V.J. (1987) Geology of the Nabarlek uranium deposit, Northern Territory, Australia. Economic Geology, 82, 1152–1168.
Windom, H., Smith, R., Niencheski, F., and Alexander, C. (2000) Uranium in rivers and estuaries of globally diverse smaller watersheds. Marine Chemistry, 68, 307–321.
Workman, R.K. and Hart, S.R. (2004) Major and trace element composition of the depleted MORB mantle (DMM). Earth and Planetary Science Letters, 231, 53–72.
Wu, W.-M. and 26 coauthors (2007) In situ bioreduction of uranium (VI) to submicromolar levels and reoxidation by dissolved oxygen. Environmental Science and Technology, 41, 5716–5723.
Yabusaki, S.B. and 10 coauthors (2007) Uranium removal from groundwater via in situ biostimulation: Field-scale modeling of transport and biological processes. Journal of Contaminant Hydrology, 93, 216–235.
Zaccarini, F., Stumpfl, E.F., and Garuti, G. (2004) Zirconolite and other Zr-Th-U minerals in chromitites of the Finero complex (Western Alps, Italy): Evidence for carbonatite-type metasomatism in a subcontinental mantle plume. Canadian Mineralogist, 42, 1463–1481.

Manuscript received February 3, 2009
Manuscript accepted May 22, 2009
Manuscript handled by Peter Dahl